Sudan University of Science and Technology

College Of Graduate Studies

Enhancement of Cervical X-ray Radiographs by Using Image Processing Technique

تحسين صور الأشعة لفقرات العنق باستخدام تقنية معالجة الصورة

A thesis Submitted for Partial Fulfillment of M.Sc. degree in Medical Physics

By:

Abdelhameed Jabir Tomba Kosti

Supervisor:

Prof. Mohamed Elfadil M. Gar-enabi

2017

الآية

بسم الله الرحمن الرحيم

قال الله تعالى:

﴿يَرْفَعِ اللَّهُ الَّذِينَ آمَنُوا مِنكُمْ وَالَّذِينَ أُوتُوا الْعِلْمَ دَرَجَاتٍ وَاللَّهُ بِمَا تَعْمَلُونَ خَبِيرٌ﴾

صدق الله العظيم

سورة المجادلة الآية (11)

Dedication

To my Father

Who always supported and encouragement me in every endeavor

My Mother

Who is reason I am here all, and me who I am today

My Brothers and Sisters

Who have provided me through moral and emotional support in my life

My Teachers and my Colleagues

I dedicate this work

Acknowledgment

Prima facie, I am grateful to the Allah for having given me patience, strength, good health and wellbeing that were necessary to accomplish this work. I send specific dept of gratitude to my supervisor,

***Prof. Mohamed Elfadil Mohamed* Gar-enabi**

for his keen supervision, patient guidance, encouragement and advice he has provided throughout my time as his student. I have been extremely lucky to have a supervisor who cared so much about my work, and who responded to my questions and queries so promptly. A special thanks goes to ***Dr. Suhaib Alameen , Mr. Abdoelrahman Hassan and Mrs. Soultana Awad***

for their kind assistance, patient helpful, useful advices and continuous encouragement.

I take this opportunity to express gratitude to all of the members of staff in ***University*** of ***Dalanj*** for their help and support.

To all my friends, Colleagues thank you for your understanding and encouragement many, many moment of crisis.

Finally, I must express my very profound gratitude to my loving parents, brothers and sisters for providing me with unfailing support and continuous encouragement throughout my years of study and through the process of researching and writing this thesis. This accomplishment would not have been possible without them. Thank you.

Abstract

Advanced technologist in image processing and analysis are used extensively in x-ray radiograph, working to improve x-ray radiographs, radiograph data are used to gather details from location of the diseases or physiological processes. This study aims to enhance cervical x-ray radiographs by using image processing technique where IDL program were used as platform to enhance the quality of the radiographs. The sampling of this study consist of 50 patient who underwent cervical x-ray radiograph, the study was conducted and taking information from Antalya Medical Center-Khartoum-Sudan, data were collected in the period between April 2017 to October 2017. IDL program techniques such as histogram equalization, filtering radiograph with mean filter, are used on this study to analyzed and enhanced data (cervical x-ray radiographs). The study showed a significant difference between the original radiograph and the radiograph that processed using IDL techniques, in term of contrast by histogram equalization. The contrast was significantly increased and it was the mean before enhancement was 0.38 and it became after filter enhancement 0.34. The mean of the signal in white area before enhancement was 920.2 and became 1308.6 after enhancement. The mean of the noise in white area before enhancement 29.7 and became 36.0 after enhancement. And the mean of signal to noise ratio in white area before enhancement was 29.7 and it became 36.0 after enhancement. Also the mean of the signal in dark area before enhancement was 1996.03 and became after enhancement 2658.6. The mean of the noise in dark area before enhancement was 44.40 and became after enhancement 51.36. And the mean of signal to noise ratio in dark area before enhancement was 44.40 and it became 51.36 after enhancement.

مستخلص البحث

التقنيات المتقدمة في معالجة الصورة وتحليلها تستخدم علي نطاق واسع في صورة الأشعة السينية و ذلك لأنها تعمل علي تحسين صورة الأشعة السينية بشكل كبير جدا أيضا يمكنها فصل المعلومات المطلوبة عن باقي الصورة، وتستخدم بيانات الصورة لجمع تفاصيل عن مكان وجود الأمراض أو العمليات الفسيولوجية. هذه الدراسة تهدف الي تحسين صورة الأشعة السينية لفقرات العنق باستخدام تقنيات معالجة الصورة حيث تم استخدام برنامج أي دي إل كمنصة لتحسين جودة الصورة. عينات هذه الدراسة تتكون من 50 مريض خضعوا لتصوير فقرات العنق بالأشعة السينية ، قد أجريت هذه الدراسة وأخذت المعلومات من مركز أنطاليا الطبي، وقد تم جمع البيانات في الفترة من مايو 2017 – أكتوبر 2017. تقنيات برنامج أي دي ال مثل تسوية الرسم البياني، ترشيح الصورة بالمرشح المتوسط، أستخدم في هذه الدراسة التحليل وتحسين صورة البيانات (الأشعة السينية لفقرات العنق). أظهرت الدراسة وجود فرق كبير بين الصورة الأصلية والصورة التي عولجت باستخدام تقنية أي دي ال، في مصطلح التباين بواسطة تسوية الرسم البياني. تمت زيادة التباين بشكل كبير وكان المتوسط قبل التحسين 0.38 وقد أصبح بعد التحسين 0.34، وكان متوسط الإشارة في المنطقة البيضاء قبل التحسين 920.2 وأصبح 1308.6 بعد التحسين. متوسط الضوضاء في المنطقة البيضاء قبل التحسين 29.7 وأصبح 36.0 بعد التحسين. وكان متوسط نسبة الإشارة إلى الضوضاء في المنطقة البيضاء قبل التحسين 29.7 وأصبح 36.0 بعد التحسين. كما أن متوسط الإشارة في المنطقة المظلمة قبل التحسين كان 1996.03 وأصبح بعد التحسين 2658.6، وكان متوسط الضوضاء في المنطقة المظلمة قبل التحسين 44.40 وأصبح بعد التحسين 51.36. وكان متوسط نسبة الإشارة إلى الضوضاء في المنطقة المظلمة قبل التحسن 44.40 وأصبح 51.36 بعد التحسين.

Tables of Contents

Topic	Page
الاية	I
Dedication	II
Acknowledgement	III
English Abstract	IV
Arabic Abstract	V
Table of contents	VI
List of tables	VII
List of figures	VIII
List of abbreviation	IX
Chapter One Introduction	
1.1 Introduction:	1
1.2 Problem of the study	7
1.3 Objectives of the Study	7
1.4 Significance of study	8
1.5 Over view of the study	8
Chapter Two Literature Review	
2.1 Anatomy of the Cervical Spine	9
2.2 Medical Imaging	11
2.3 Image Processing	11
2.3.1 Analog Image Processing	11
2.3.2 Digital Image Processing	12
2.4 Steps of Image Processing	13
2.5 Type of Digital Images	14
2.6 Advanced Digital Image processing Techniques	16
2.7 Image Analysis	17
2.8 Image Restoration:	17
2.9 Physical-technical image quality parameters	18
2.10 Image Enhancement Techniques	20
2.10.1 Filters	25
2.10.2 Contrast	25

2.10.3 Contrast enhancement	25
2.10.4 Histogram Modification	30
2.11 Texture	31
2.12 IDL in image processing	33
2.13 Previous of Studies	35
Chapter Three **Material & Methodology**	
3.1 Material	42
3.2 Methods	43
3.2.1 Place and duration of the Study	43
3.2.2 Study Population	43
3.2.3 Study design	43
3.2.4 Sampling and type	43
3.3 Method of data collection	43
3.4 Method of data presentation	44
3.5 Method of data analysis	44
Chapter Four **Results and Analysis**	
The Results	45
Chapter Five **Discussion, Conclusions and Recommendations**	
5-1 Discussion	53
5-2 Conclusion	56
5-3 Recommendations	57
References	58
Appendix	

List of tables

Table No.	Title	Page
3-1	feature of the X-ray machine	42
4-1	the mean and standard deviation in White area before and after enhancement	49
4-2	the mean and standard deviation in dark area before and after enhancement	51
4-3	Shows the mean and standard for contrast before and after enhancement	52

List of figures

Figure	Title	Page
Fig. 1-1	Components of X-ray	3
Fig. 2-1	AP views of the Adult Cervical Spine	10
Fig. 2-2	Lateral views of the Adult Cervical Spine	10
Fig. 2-3	Basic Principles of Digital Image Processing	13
Fig. 2-4	The effect of digitization	16
Fig. 2-5	(a) Example of original cervical radiograph. (b) Enhanced cervical radiograph after adaptive histogram equalization	22
Fig. 2-6	Unsharp masking applied after adaptive histogram equalization. The two-dimensional, zero-mean discrete Gaussian function is defined by equation (2.1), where the standard deviation, σ , determines the width of the Gaussian	22
Fig. 2-7	(a) A section of original X-ray image of cervical vertebra. (b) Enhanced image after adaptive histogram equalization, (c) Enhanced image after adaptive histogram equalization and unsharp masking, (d) Enhanced image after applying 3rd Derivative of Gaussian separable steerable filters ($\mu = 0.09, \sigma = 1.5$).	24
Fig. 2-8	Interpolation applied to zooming an image by a factor of two	28
Fig. 2-9	Digital images of two visibly different textured regions extracted from the Brodatz texture database (Brodatz, 1966). Left, image of grass (1.2.01, D9 H.E.). Right, image of water (1.2.08, D38 H.E.) (Weber, 2004).	33
Fig. 3-1	Demonstrated X-Ray Machine Line Frequency	42
Fig. 4-1	demonstrated original radiographs for cervical spine (A) the original radiograph (B) showed radiograph after Histogram equalization. (C) Showed an radiograph after median filter smoothing.	45
Fig. 4-2	Simple error bar demonstrate the difference in signal in the white(w) and dark(d) area before(B) and after(A) enhancement	46
Fig. 4-3	Simple error bar demonstrate the difference in noise in the white(w) and dark(b) area before(B) and after(A) enhancement	46

Fig. 4-4	Simple error bar demonstrate the difference in signal/noise ratio before and after enhancement	47
Fig. 4-5	Simple error bar demonstrate the difference in contrast in white and dark area before and after enhancement	47
Fig. 4-6	the relationship between signal in white area before and after enhancement area before and after enhancement	48
Fig. 4-7	the relationship between noise in white area before and after enhancement	48
Fig. 4-8	the relationship between signal to noise ratio in white area before and after enhancement	49
Fig. 4-9	the relationship between signal in dark area before and after enhancement	50
Fig. 4-10	the relationship between noise in dark area before and after enhancement	50
Fig. 4-11	the relationship between signal to noise ratio in dark area before and after enhancement	51
Fig. 4-12	the relationship between contrast before and after enhancement	52

List of abbreviations

Abbr.	Title
OCR	optical character recognition
RGB	Red green blue
NDT	Non destructive test
m	Number of the columns of the image matrix
n	Number of the rows of the image matrix
BMP	Bitmap
JPEG	Joint Photographic Experts Group
TIFF	Tagged Image File Format
NPS	Noise power spectrum
ROI	Region of Interest
IR	Iterative Reconstruction
MTF	Modulation transfer function
DQE	Detective quantum efficient
CNR	Contrast to Noise Ratio
GSM	Gaussian Scale Mixture
BLS	Bayesian Least Squares
SPECT	Single Photon Emission Computed Tomography
PET	Positron Emission Tomography
BYTSCL	Byte-Scaling
SNR	Signal-to-Noise Ratio
IDL	Interactive Data Language
GL	Gray level
GUI	Graphical User Interface
PDE	Partial Differential Equations
PSNR	Peak Signal-to-Noise Ratio
VLSI	Very-large-scale integration
FPGA	Field-programmable gate array
CTV	Color Total Variation
EME	Measure of Enhancement
IPT	Image Processing Toolbox
AH	Adaptive Histogram
MSR	Multi-scale Retinex
BPNN	Back Propagation Neural Networks

SVM	Support Vector Machine
NB	Naïve Bayes
CLAHE	Contrast limited adaptive histogram equalization
PC	Personal Computer
DICOM	Digital Imaging and Communications in Medicine
HE	Histogram equalization
CR	computed radiograph

CHAPTER ONE

Chapter One

1.1. Introduction

X-rays are among the oldest sources of EM radiation used for imaging. The best known use of X-rays is medical diagnostics, but they also are used extensively in industry and other areas, like astronomy. X-rays for medical and industrial imaging are generated using an X-ray tube, which is a vacuum tube with a cathode and anode. The cathode is heated, causing free electrons to be released. These electrons flow at high speed to the positively charged anode. (Gonzalez et al, 2008).

When the electrons strike a nucleus, energy is released in the form of X-ray radiation. The energy (penetrating power) of X-rays is controlled by a voltage applied across the anode, and by a current applied to the filament in the cathode. The intensity of the X-rays is modified by absorption as they pass through the patient, and the resulting energy falling on the film develops it, much in the same way that light develops photographic film. In digital radiography, digital images are obtained by one of two methods by digitizing X-ray films, or by having the X-rays that pass through the patient fall directly onto devices (such as a phosphor screen) that convert X-rays to light. The light signal in turn is captured by a light-sensitive digitizing system. (Gonzalez et al, 2008).

An x-ray is a discrete bundle of electromagnetic energy called a photon. In that regard, it is similar to other forms of electromagnetic energy such as light, infrared, ultraviolet, radio waves, or gamma rays. The associated electromagnetic energy can be thought of as oscillating electric and magnetic fields propagating through space at the speed of light. The various forms of electromagnetic energy differ only in frequency (or wavelength). However, because the energy carried by each photon is

proportional to the frequency (the proportionality constant is called Planck's constant), the higher frequency x-ray or gamma ray photons are much more energetic than, for example, light photons and can readily ionize the atoms in materials on which they impinge. The energy of a light photon is of the order of one electron-volt (eV), whereas the average energy of an x-ray photon in a diagnostic x-ray beam is on the order of 30 kiloelectron volts (keV) and its wavelength is smaller than the diameter of an atom (10_8 cm). In summary, an x-ray beam can be thought of as a swarm of photons traveling at the speed of light, each photon representing a bundle of electromagnetic energy. (Chen et al. 2011).

Electromagnetic radiation may be produced in a variety of ways. One method is the acceleration or deceleration of electrons. For example, a radio transmitter is merely a source of high-frequency alternating current that causes electrons in an antenna wire to which it is connected to oscillate (accelerate and decelerate), thereby producing radio waves (photons) at the transmitter frequency. In an x-ray tube, electrons boiled off from a hot filament figure (1-1) are accelerated toward a tungsten anode by a high voltage on the order of 100 kilovolts(kV). Just before hitting the anode, the electrons will have a kinetic energy in kiloelectron volts equal in magnitude to the kilo voltage (e.g. if the voltage across the x-ray tube is 100 kV, the electron energy is 100 keV).When the electrons smash into the tungsten anode, most of them hit other electrons, and their energy is dissipated in the form of heat. In fact, the anode may become white-hot during an x-ray exposure, which is one reason for choosing an anode made of tungsten, with a very high melting point. (Chen et al. 2011).

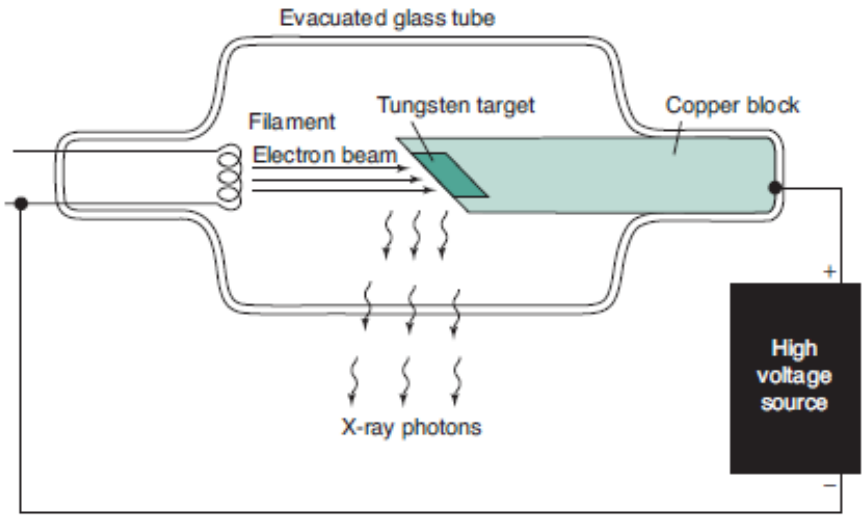

Figure: (1-1): Components of X-ray. (Chen et al. 2011)

The electrons penetrate the anode to a depth less than 0.1 mm. A small fraction of the electrons, however, may have a close encounter with a tungsten nucleus, which, because of its large positive charge, exerts a large attractive force on the electron, giving the electron a hard jerk (acceleration) of sufficient magnitude to produce an x-ray photon. The energy of the x-ray photon, which is derived from the energy of the incident electron, depends on the magnitude of the acceleration imparted to the electron. The magnitude of the acceleration, in turn, depends on how closely the electron passes by the nucleus. If one imagines a target consisting of a series of concentric circles, such as a dart board, with the bull's-eye centered on the nucleus, more electrons clearly will impinge at larger distances than in the bull's-eye; hence, a variety of x-ray photon energies will be produced at a given tube voltage (kV) up to a maximum equal to the tube voltage (a hit in the bull's-eye), where the electron gives up all its energy to the x-ray photon. Increasing the voltage will shift the x-ray photon spectrum to higher energies, and higher-energy photons are more penetrating. (Chen et al. 2011).

The radiation produced in this manner is called Bremsstrahlung (braking radiation) and represents only about 1% of the electron energy dumped into the anode by the electron beam; the other 99% goes into heat. The electron current from filament to anode in the x-ray tube is called the mA, because it is measured in milliamperes. The mA is simply a measure of the number of electrons per second making the trip across the x-ray tube from filament to anode. The rate of x-ray production (number of x-rays produced per second) is proportional to the product of milliamperage and kilo voltage squared. The quantity of x-rays produced in an exposure of duration s (in seconds) is proportional to the product of mA and time and is called the mAs. The quantity of x-rays at a given point is generally measured in terms of the amount of ionization per cubic centimeter of air produced at that point by the x-rays and is measured in roentgens (R) or in coulombs per kilogram of air. This quantity is called exposure, and 1 R of exposure results in 2 _ 109 ionizations per cubic centimeter of air. The electron beam is made to impinge on a small area on the anode of the order of 1 mm in diameter in order to approximate a point source of x-rays. Because a radiograph is a shadow picture, the smaller the focal spot, the sharper the image. By analogy, a shadow picture on the wall (such as a rabbit made with one's hand) will be much sharper if a point source of light such as a candle is used rather than an extended light source such as a fluorescent tube. The penumbra (or unsharpness) of the shadow will depend not only on the source size, but also on the magnification, as can be illustrated by making a shadow of one's hand on a piece of paper using a small light source such as a single light bulb. (Chen et al. 2011).

The closer you bring your hand to the paper (the smaller the magnification), the sharper the edges of the shadow. Similarly, magnification of the x-ray image produced by the point source is less, the closer the patient is to the film and the farther the source is from the film.

The magnification factor (M) is defined as the ratio of image size to object size and is equal to the ratio of the focal-to-film distance divided by the focal to object distance (M _ 1, and M _ 1 means no magnification is produced; ie, either the object is right against the film, or the focal spot is infinitely far away). The penumbra, blurring, or unsharpness (_x) produced on an otherwise perfectly sharp edge of an object and due to the finite focal spot size of dimension *a* is expressed by the equation _*x* _ *a*(*M* _ 1) Unfortunately, the smaller the focal spot, the more likely it is that the anode will melt. The power (energy/per second) dumped into the anode is equal to the product of the kilovoltage and milliamperage; ie, at 100 kV and 500 mA, 50,000 watts of heat energy is deposited into an area on the order of a few square millimeters (imagine a 50,000-watt light bulb to get an idea of the heat generated). (Chen et al. 2011).

Medical imaging of the human body requires some form of energy. In the medical imaging techniques used in radiology, the energy used to produce the image must be capable of penetrating tissues. Visible light, which has limited ability to penetrate tissues at depth, is used mostly outside of the radiology department for medical imaging. Visible light images are used in dermatology (skin photography), gastroenterology and obstetrics (endoscopy), and pathology (light microscopy). Of course, all disciplines in medicine use direct visual observation, which also utilizes visible light. In diagnostic radiology, the electromagnetic spectrum outside the visible light region is used for x-ray imaging, including mammography and computed tomography, magnetic resonance imaging, and nuclear medicine. Mechanical energy, in the form of high-frequency sound waves, is used in ultrasound imaging. (Bushberg, 2002).

While medical images can have an aesthetic appearance, the diagnostic utility of a medical image relates to both the technical quality of the image and the conditions of its acquisition. Consequently, the assessment

of image quality in medical imaging involves very little artistic appraisal and a great deal of technical evaluation. In most cases, the image quality that is obtained from medical imaging devices involves compromise-better x-ray images can be made when the radiation dose to the patient is high, better magnetic resonance images can be made when the image acquisition time is long, and better ultrasound images result when the ultrasound power levels are large. Of course, patient safety and comfort must be considered when acquiring medical images; thus excessive patient dose in the pursuit of a perfect image is not acceptable. Rather, the power levels used to make medical images require a balance between patient safety and image quality. (Bushberg, 2002).

Image Enhancement is simple and most appealing area among all the digital image processing techniques. The main purpose of image enhancement is to bring out detail that is hidden in an image or to increase contrast in a low contrast image. Histogram equalization is one of the well known image enhancement technique. HE becomes a popular technique for contrast enhancement because this method is simple and effective. To display a digital image, pixel values from the minimal pixel value to the maximal value in the image must be displayed. For displaying the image, a range of video intensities from the darkest to the brightest the video monitor can produce is available. There is a great amount of choice in how the mapping from pixel value to video intensity is to be performed. Selecting a mapping that optimizes the display of important features in the image is called contrast enhancement. There are two methods for contrast enhancement available on most medical image-processing computers: translation table selection and windowing. Both of these may be considered to be methods image processing. (Chen et al, 2011).

It accentuates or sharpens image features such as edges, boundaries, or contrast to make a graphic display more helpful for display and analysis. The enhancement doesn't increase the inherent information content of the data, but it increases the dynamic range of the chosen features so that they can be detected easily. (Bushberg, 2002).

1.2. Problem of the study:

Cervical images as 2D image format make all the structures in the cervical superimposed. Also medical images are often deteriorated by noise due to various interferences and other factor associated with imaging process and data acquisition system. This will make the visibility of normal and abnormal structure as difficult to be demonstrated, using image processing technique to enhance the image will improve the visibility of image textures in a way that it can gives optimum diagnostics workup.

1.3. Objectives of the study:

1.3.1. General objective:

The main objective of this study was to enhance cervical images by using image processing techniques in order to increase the visual perception characteristics.

1.3.2. Specific objectives:

- To enhance the cervical images using histogram equalization function and median filter.
- To calculate the contrast, noise, signal and signal to noise ratio for cervical images before and after enhancement and filtering.
- To find the enhancement coefficient function using contrast, noise, signal and signal to noise ratio.
-

1.4. Significance of study:

This study was provided to improve the cervical images using filtering by revealing the effect of enhancement and reduction of noise and hence increasing signal to noise ratio and therefore contrast of the image.

1.5. Overview of the study:

This study falls into five chapters, chapter one, which is an introduction, deals with theoretical frame work of the study and it presents the statement of the study problems, objectives of the study and significant, chapter two deals with radiological physics, back ground and previous studies (literature review), chapter three deals with materials and methods, chapter fours present result and finally chapter five deals with discussion, conclusion, and recommendations.

CHAPTER TOW

Chapter Two

Literature Review

2.1 Anatomy of the Cervical Spine:

The Cervical spine (C-spine) consists of seven vertebrae (C1–C7) and supports the weight of the head (approximately 14 pounds). The first two vertebrae are called the axis and atlas, respectively, and do not have a disc between them, but are closely bound to gether by a complex of ligaments. The C1 (axis) "ring" rotates around the odontoid or "peg" of C2 (atlas), allowing for almost 50% of total cervical rotation. The spinal canal is housed within the cervical vertebrae and is widest between the C1 and C3levels (A-P diameter 16–30 mm) and narrows as it progresses caudally (14–23 mm). When the neck is fully extended, this canal can narrow an additional 2–3 mm. cervical spine vertebrae differ from lumbosacral vertebrae in several ways. First, there are foramina on each side which allow passage of the vertebral arteries. Additionally, the facet joints in the C-spine have steeper angles which allow formore rotation between vertebrae without subluxation. The most important difference, however, is the non synovial joint, known as the uncovertebral joint or "joint of Luschka." During midlife, this joint prevents a disc rupture from directly pressingonto the nerve root. This means that most disc herniations in the neck occur posteriorly (unlike the LS spine, in which most herniations occur laterally). As we age, these joints can form osteophytes that can impinge upon the nerve rootor compress the cervical cord directly causing cervical myelopathy. (Deen et al, 1992).

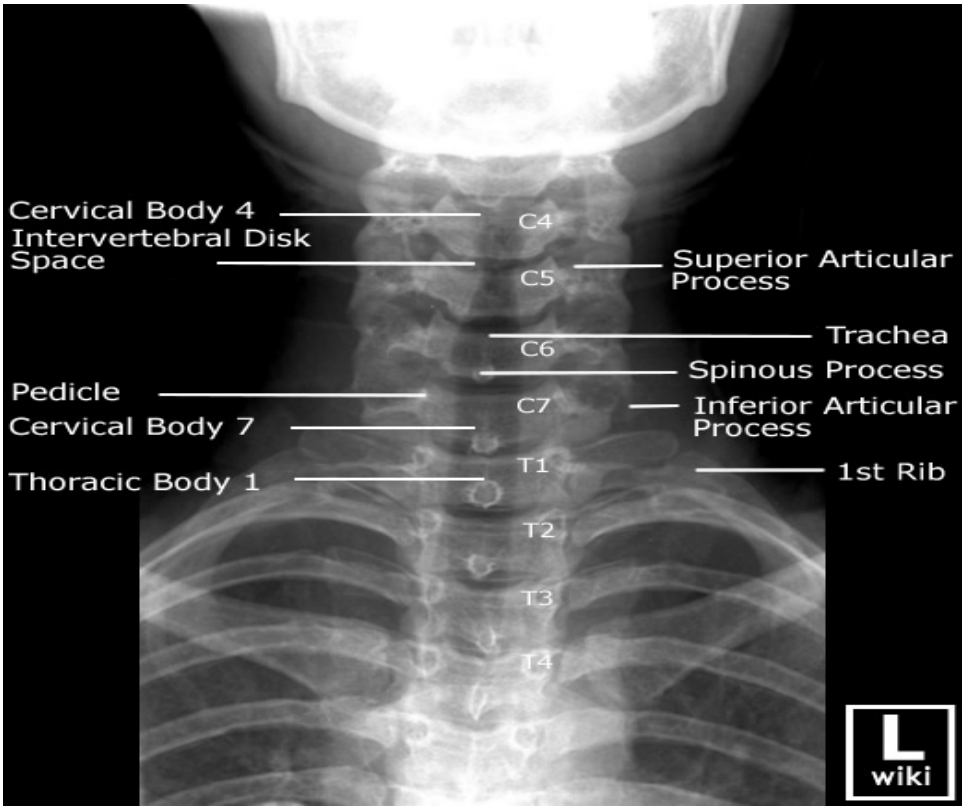

Figure (2-1): AP views of the Adult Cervical Spine (Deen et al, 1992)

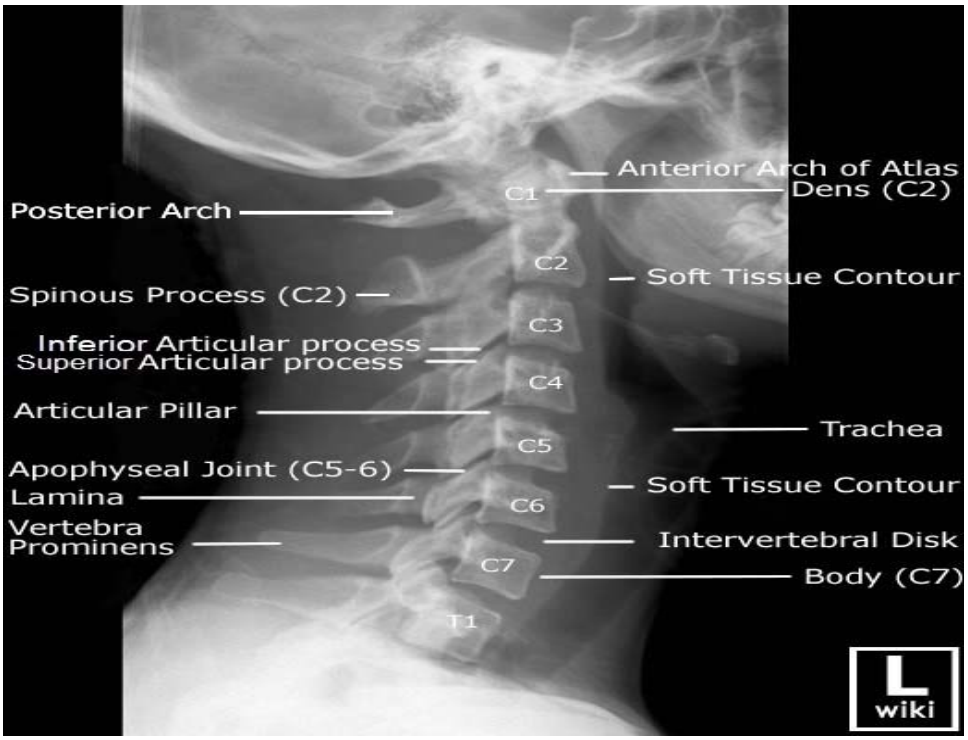

Figure (2-2): Lateral views of the Adult Cervical Spine (Deen et al, 1992)

2.2 Medical Imaging:

Imaging technology in Medicine made the doctors to see the interior portions of the body for easy diagnosis. It also helped doctors to make keyhole surgeries for reaching the interior parts without really opening too much of the body. CT Scanner, Ultrasound and Magnetic Resonance Imaging took over x-ray imaging by making the doctors to look at the body's elusive third dimension. With the CT Scanner, body's interior can be bared with ease and the diseased areas can be identified without causing either discomfort or pain to the patient. MRI picks up signals from the body's magnetic particles spinning to its magnetic tune and with the help of its powerful computer, converts scanner data into revealing pictures of internal organs. Image Processing techniques developed for analyzing remote sensing data may be modified to analyze the outputs of medical imaging systems to get best advantage to analyze symptoms of the patients with ease. (Deserno et al, 2011).

2.3 Methods of Image Processing:

2.3.1 Analog Image Processing:

Analog Image Processing refers to the alteration of image through electrical means. The most common example is the television image.

The television signal is a voltage level which varies in amplitude to represent brightness through the image. By electrically varying the signal, the displayed image appearance is altered. The brightness and contrast controls on a TV set serve to adjust the amplitude and reference of the video signal, resulting in the brightening, darkening and alteration of the brightness range of the displayed image. (Gonzalez et al, 2008).

2.3.2 Digital Image Processing:

An image may be defined as a two-dimensional function, where x and Y are spatial(plane) coordinates, and the amplitude of fat any pair of coordinates (x,y) is called the intensity or gray level of the image at that point. When x, y, and the intensity values of fare all finite, discrete quantities, we call the image a digital image. The field of digital image processing refers to processing digital images by means of a digital computer. Note that a digital image is composed of a finite number of elements, each of which has a particular location and value. These elements are called picture elements, image elements, pels, andpixels. Pixel is the term used most widely to denote the elements of a digital image. (Gonzalez et al, 2008).

Image processing is a method to convert an image into digital form and perform some operations on it, in order to get an enhanced image or to extract some useful information from it. It is a type of signal dispensation in which input is image, like video frame or photograph and output may be image or characteristics associated with that image. Usually Image Processing system includes treating images as two dimensional signals while applying already set signal processing methods to them. It is among rapidly growing technologies today, with its applications in various aspects of a business. Image Processing forms core research area within engineering and computer science disciplines too. (Tinku, Ajoy K, 2005).

Digital Processing the general digital image processing system may be divided into three components: the input device (or digitizer), the digital processor, and the output device (image display). The digitizer converts a continuous-tone and spatially continuous brightness distribution f[x,y] to an discrete array (the digital image) fg[n, m], where n, m, and fq are integers, The digital processor operates on the digital imagefg[n, m] to

generate a new digital image gq[k, c], where k, c, and gq are integers. The output image may be represented in a different coordinate system, hence the use of different indices k and c. and the image display converts the digital output image Gq[k, c] back into a continuous one and spatially continuous image g[x, y] for viewing. It should be noted that some systems may not require a display (e.g., in machine vision and artificial intelligence applications); the output may be a piece of information. (Easton 2010).

Image Processing systems are becoming popular due to easy availability of powerful personnel computers, large size memory devices, graphics soft wares etc.(Deserno et al, 2011).

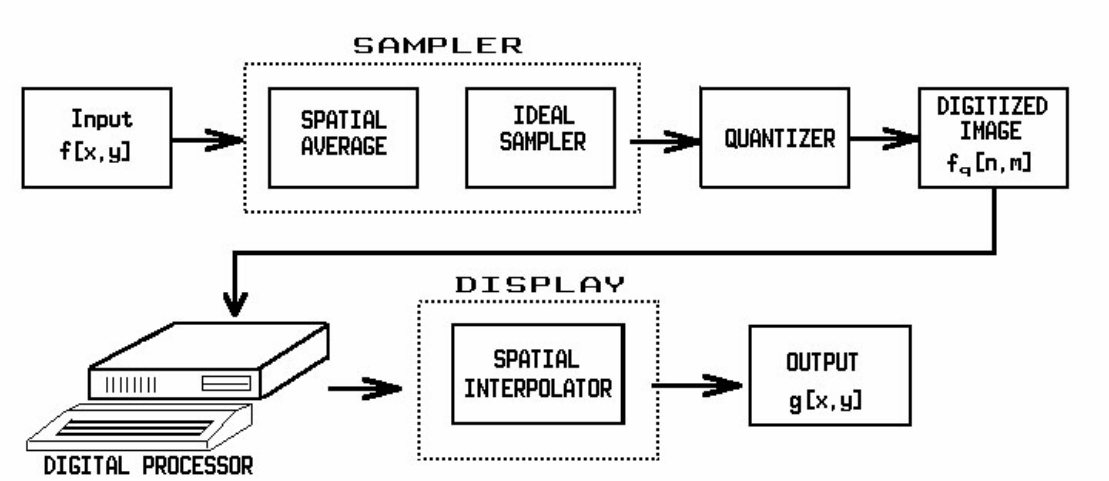

Figure (2-3): Basic Principles of Digital Image Processing. (Easton et al, 2010).

2.4 Steps of Image Processing:

The commonly used term "biomedical image processing" means the provision of digital image processing for biomedical sciences. In general, digital image processing covers four major areas: Image formation includes all the steps from capturing the image to forming a digital image matrix, Image visualization refers to all types of manipulation of this

matrix, resulting in an optimized output of the image. And Image analysis includes all the steps of processing, which are used for quantitative measurements as well as abstract interpretations of biomedical images. These steps require a priori knowledge on the nature and content of the images, which must be integrated into the algorithms on a high level of abstraction. Thus, the process of image analysis is very specific, and developed algorithms can be transferred rarely directly into other application domains. And Image management sums up all techniques that provide the efficient storage, communication, transmission, archiving, and access (retrieval) of image data. Thus, the methods of telemedicine are also a part of the image management. In contrast to image analysis, which is often also referred to as high-level image processing, low-level processing denotes manual or automatic techniques, which can be realized without a priori knowledge on the specific content of images. This type of algorithms has similar effects regardless of the content of the images. For example, histogram stretching of a radiograph improves the contrast as it does on any holiday photograph. Therefore, low-level processing methods are usually available with programs for image enhancement (Deserno et al, 2011).

2.5 Type of Digital Images:

The images types we will consider are: binary, gray-scale, color and multispectral.

Binary images: Binary images are the simplest type of images and can take on two values, typically black and white, or 0 and 1. A binary images is referred to as a 1-bit image because takes only 1 binary digital to represent each pixel. These types of images are frequently used in applications where the only information required is general shape or

outline. For example optical character recognition (OCR).Binary images are often created from the gray-scale images via a threshold operation, where every pixel above the threshold value is turned white ('1'), and those below it are turned black ('0').(Rao et al, 2006).

Gray-Scale Images: Gray-scale images are referred to as monochrome (one-color) image They contain gray-level information. No color information. The number of bit used for each pixel determines the number of different gray levels available. The typical gray-scale image contains 8bits/pixel data, which allows us to have 256 different gray level .In application like medical imaging and astronomy. 12 or 16 bits/pixel images are used. These extra gray levels become useful when a small section of the image in made much larger to discern details. (Rao D. V. G. L. N et al, 2006).

Color images: Color images can be modeled as three-band monochrome image data, where each band of data corresponds to a different color. The actual information stored in the digital image data is the gray-level information in each spectral band. Typical color images are represented as red, green and blue (RGB images). Using the 8-bit monochrome standard as model. The corresponding color image would have 24-bits/pixel (8-bits for each of the three color bands red, green and blue). (Rao D. V. G. L. N et al, 2006).

Multispectral images: Multispectral images typically contain information outside the normal human perceptual range. This may include infrared, ultraviolet, X-ray acoustic, or radar data. These are not images in the usual sense because the information represented is not directly in the visible by the human system. However, the information is often represented visual form by mapping the different spectral band to RGB components. (Rao et al, 2006).

2.6 Advanced Digital Image Processing Techniques:

Neural Network based Image Processing, Statistical approach for texture analysis, Segmentation in color and band width (B/W) images, Expert system based Image Processing, Application of object oriented programming techniques in Image Processing environments, Shape in machine vision, Multispectral classification techniques, Auto focusing techniques for MRI images, Thresholding technique for finding contours of objects, Sequential segmentation technique to find out thin vessels in medical images and hair line cracks in NDT, Fractal method for texture classification, Data compression techniques using fractals and Discrete Cosine Transformers and Image restoration methods using Point Spread functions and Wiener filter etc. (Rao et al, 2006).

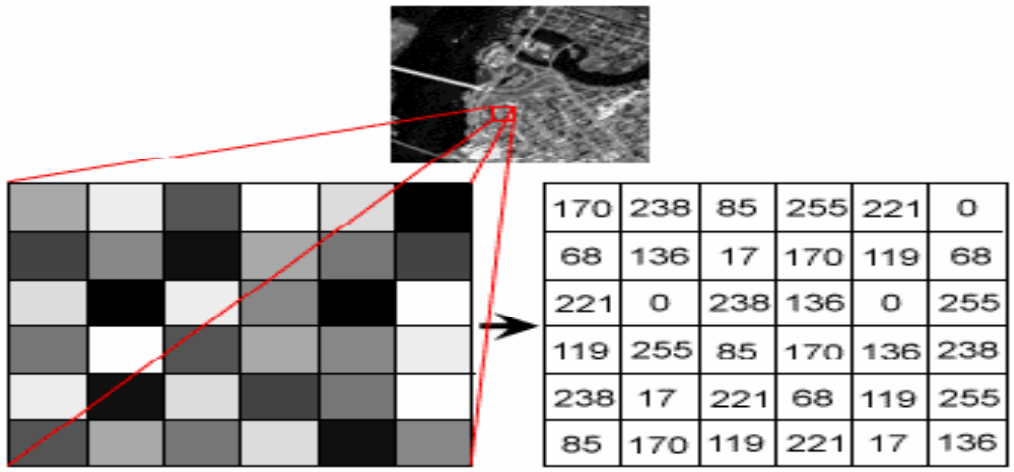

Figure (2-4): The effect of digitization. (Rao et al, 2006).

The 2D continuous image *f (x,y)* is divided into N rows and M columns. The intersection of a row and a column is called as *pixel*. The value assigned to the integer coordinates [*m*, *n*] with {*m*=0,1, 2,...,*M*-1} and {*n*=0,1,2,...,*N*-1} is *f*[*m*, *n*]. In fact, in most cases *f*(*x*, *y*)--which we might consider to be the physical signal that impinges on the face of a sensor. Typically an image file such as BMP, JPEG, TIFF etc., has some header

and picture information. A header usually includes details like format identifier (typically first information), resolution, number of bits/pixel, compression type, etc. (Rao et al, 2006).

2.7 Image Analysis:

Image analysis is concerned with making quantitative measurements from an image to produce a description of it. In the simplest form, this task could be reading a label on a grocery item, sorting different parts on an assembly line, or measuring the size and orientation of blood cells in a medical image. More advanced image analysis systems measure quantitative information and use it to make a sophisticated decision, such as controlling the arm of a robot to move an object after identifying it or navigating an aircraft with the aid of images acquired along its trajectory.

Image analysis techniques require extraction of certain features that aid in the identification of the object. Segmentation techniques are used to isolate the desired object from the scene so that measurements can be made on it subsequently. Quantitative measurements of object features allow classification and description of the image. (Raghuveer M et al, 2004).

2.8 Image Restoration:

Image restoration refers to removal or minimization of degradations in an image. This includes de-blurring of images degraded by the limitations of a sensor or its environment, noise filtering, and correction of geometric distortion or non-linearity due to sensors. Image is restored to its original quality by inverting the physical degradation phenomenon such as defocus, linear motion, atmospheric degradation and additive noise. (Raghuveer M et al, 2004).

2.9 Physical-technical image quality parameters:

Noise: Noise and noise related properties of a radiological image are of great importance to diagnostic performance. Noise is based on the standard deviation of pixel values in an image, while NPS is a metric of image quality used to measure the noise characteristics and patterns in all frequencies of the image. In this way NPS provides us with a more complete description of noise in an image. Noise and noise related parameters are used for many applications, such as benchmarking image quality across systems, optimizing acquisition and reconstruction parameters to improve dose efficiency, and predicting observer performance. The question is of course if the properties of noise and NPS are suitable to draw such type of conclusions. The detection of lesions or abnormalities in medical images is impaired greatly by the presence of image noise. One component of medical image noise is quantum noise, the variability in the image's intensity distribution due to the statistical fluctuations in the number of photons reaching the image receptor. A second component of medical image noise is anatomical noise, which originates from anatomic structures in the image that are irrelevant to the detection. Noise and noise related properties are quantified on structure-free images which implies that the radiological task of detection of lesions or abnormalities is quantum noise limited rather than limited by the projected anatomy. This assumption is obviously not true for many common tasks in diagnostic radiology. Furthermore, when the anatomical noise dominates, the image quality depends less on the dose than expected from quantum noise considerations. (Thierens et al, 2017).

Another drawback of using noise as an image quality parameter is that noise is commonly estimated over a ROI in a single image, employing assumptions of linearity and stationarity. However, in newly developed reconstruction methods as iterative reconstruction (IR), the system is

potentially nonlinear which implicates that noise is highly spatially dependent and that image resolution depends on contrast. So the evaluation of noise and resolution depends on the properties of the imaging task. As a result, task-independent metrics such as noise or NPS are no longer adequate for evaluations of IR image quality. (Thierens et al, 2017).

Resolution: The evaluation of spatial resolution of imaging systems plays a central role in imaging performance evaluation. One of the most comprehensive metrics used to measure and report spatial resolution of imaging systems is the MTF. The MTF provides a measure of how well the system transfers contrast across spatial-frequencies. The MTF is also essential to evaluating other key imaging performance metrics such as the DQE. The MTF is a useful quantity for linear systems, where the imaging system's response to an arbitrary object can be determined by convolving the true object and the point spread function. This is not true for nonlinear IR algorithms. As the MTF is not well defined for images reconstructed by IR, it is of limited utility in assessing the quality of these images. The introduction of iterative reconstruction systems has posed a challenge in our ability to assess spatial resolution. Current MTF assessment methods only focus on linear systems with a single contrast and noise level. (H. Thierens et al, 2017).

Contrast: The CNR is a useful metric for describing the signal amplitude relative to the ambient noise for simple and largely homogeneous objects. However, the CNR depends only on contrast and noise. Actual signal detectability also depends on factors including signal size, shape and density distribution; background level, variability and correlation; the variance and covariance of measurement noise; spatial resolutions; and the observer and detection strategy used. The CNR can be useful in some simple situations, e.g. determining thresholds of contrast agents at which

signals on a test phantom become visible. However, the CNR is in general not a complete description of an observer's ability to detect lesions, and this is even more true for IR images which are more likely to be nonlinear and nonstationary. (Thierens et al, 2017).

2.10 Image Enhancement Techniques:

Image enhancement techniques improve the quality of an image as perceived by a human. These techniques are most useful because many satellite images when examined on a color display give inadequate information for image interpretation. There is no conscious effort to improve the fidelity of the image with regard to some ideal form of the image. There exists a wide variety of techniques for improving image quality. The contrast stretch, density slicing, edge enhancement, and spatial filtering are the more commonly used techniques. Image enhancement is attempted after the image is corrected for geometric and radiometric distortions. Image enhancement methods are applied separately to each band of a multispectral image. Digital techniques have been found to be most satisfactory than the photographic technique for image enhancement, because of the precision and wide variety of digital processes. Typically, digitized X-ray images are corrupted by additive noise. De-noising can improve the visibility of some structures in medical X-ray images, thus improving the performance of computer assisted segmentation algorithms. However, image enhancement algorithms generally amplify noise. Therefore, higher de-noising performance is important in obtaining images with high visual quality. The most important part of the corrupting noise is the spatially correlated Gaussian noise whose variance may vary with the signal level due to sensor non-linearity. There exists different adaptive image enhancement methods, such as adaptive unsharp masking, adaptive neighborhood filtering and enhancement, adaptive contrast enhancement, and various adaptive

filtering approaches using directional wavelet transform. Some methods require a priori information about the image. (Cheng, 2006).

Adaptive histogram-based equalization can be applied to aid in the viewing of key cervical and lumbar vertebrae features. However, since the method was applied to the entire image where areas including the skull and shoulders biased the histogram with a large number of high gray levels, the resulting enhancement often yielded poorly contrast enhanced vertebrae near these areas. For example, Figure 2.5(a) shows an original cervical X-ray image and Figure 2.5(b) the corresponding image after adaptive histogram equalization with C7 distorted. The vertebrae C1, C2 and C7are basically left out because these structures are often not visible on the radiograph29and hence it is difficult to characterize them. Thus the regions of interest for segmentation are the cervical vertebrae (C3 to C6) and the lumbar vertebrae (L1 toL5) showed in Figures 2.5(c) and (d).For some images, adequate contrast enhancement may not be achieved using only adaptive histogram equalization. Unsharp masking was further applied on the histogram-equalized cropped portion of the image. As shown in Figure 2.6, the main idea is to subtract the smoothed image section filtered by a Gaussian filter with a large standard deviation, large σ, from the smoothed version filtered by a Gaussian filter with a small standard deviation, small σ. This operation will cancel any subtle variation in the gray scale, preserving only abrupt changes (edges). The parameters of the standard deviation of the Gaussian mask small σ and large σ have been fixed respectively for cervical and lumbar images to achieve better enhancement performance. An example of the enhanced image using only adaptive histogram equalization is shown in (Figure 2.7(b)), and the enhanced image processed by both histogram equalization and unsharp masking is shown in (Figure 2.7(c)). (Cheng, 2006).

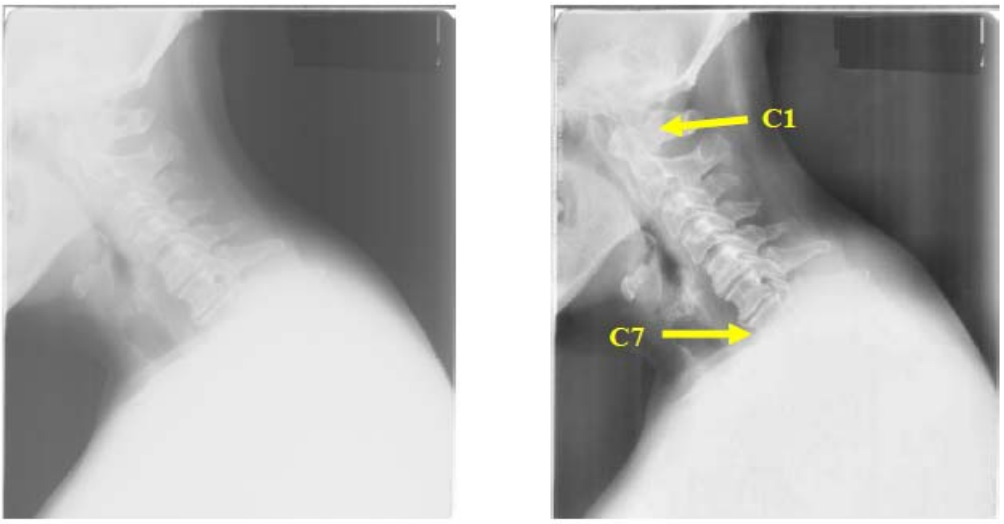

Figure (2-5): (a) Example of original cervical image. (b) Enhanced cervical image after adaptive histogram equalization. (Cheng, 2006).

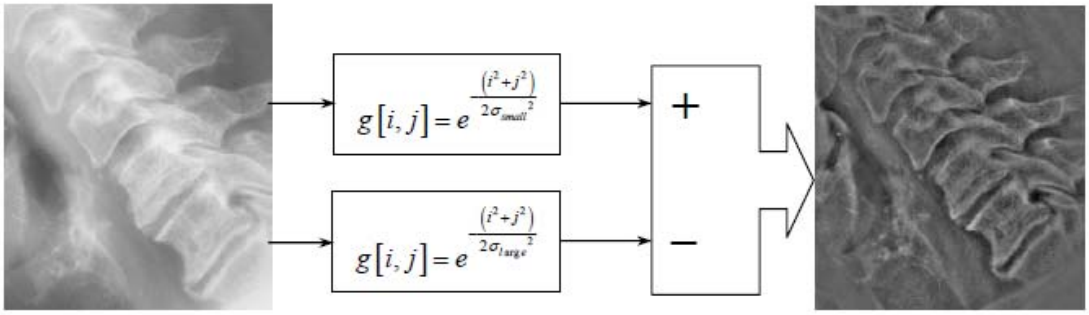

Figure (2-6): Unsharp masking applied after adaptive histogram equalization. The two-dimensional, zero-mean discrete Gaussian function is defined by equation (2.1), where the standard deviation, σ , determines the width of the Gaussian. (Cheng, 2006).

$$g[x,y]=\exp\left(-\frac{(x^2+y^2)}{2\sigma^2}\right) \qquad \text{.....(2.2)}$$

The degree of smoothing of a Gaussian filter is controlled by the parameter σ. Large σ implies a wider Gaussian filter and enhanced

smoothing effect. And the amount of smoothing by Gaussian filters will be the same in all directions. The steerable filter can also be applied to assist in the viewing of key cervical and lumbar vertebrae features. It is an efficient process for removing noise and enhancing oriented structures by angular adaptive filtering. We used the steerable properties of derivatives of Gaussians for image enhancement. Figure 2.10(d)) shows the result of filtering with a 3rd derivative of Gaussian separable steerable filters ($\mu = 0.09, \sigma = 1.5$). (Cheng, 2006).

Another important issue with image enhancement is to remove unwanted noise from the available edge image. This objective can be achieved using a great variety of algorithms and, consequently, the different algorithms that this particular approach uses can be substituted for any other that yield similar or better results. We assume that the image is corrupted by independent additive white Gaussian noise of known variance. This specific de-noising approach uses the same top-level structure as most approaches: decompose the image into pyramid sub ands at different scales and orientations; de-noise each sub and, except for the low pass residual band; invert the pyramid transform to reconstruct the de-noised image from the processed sub ands and the low pass residual. The main features of the method are that the coefficients within each local neighborhood around a reference coefficient of a pyramid sub and are characterized by a Gaussian Scale Mixture (GSM) model. Second, a statistical model of the coefficients of an over complete multi-scale oriented basis was used, and the Bayesian least squares estimate of each coefficient was reduced to a weighted average of the local linear estimate over all possible values of the hidden multiplier variable under this model. Figure (2.11) shows an example of first de-nosing the image, then applying the Canny edge detector to obtain the binary edge information. The BLS-GSM de-noising method reduced the amount of

unwanted high frequency components that appear in the form of small broken edges but retained most long edge information. For various de-noising and image enhancement methods, one important issue to be considered is computational efficiency. The algorithm should be executable in are as on able time, since the number of human experts is limited and the workloads of radiological units are increasing especially due to the screening policies. The accuracy and resolution of X-ray images are also increasing, thus requiring more computations to be performed. (Cheng, 2006).

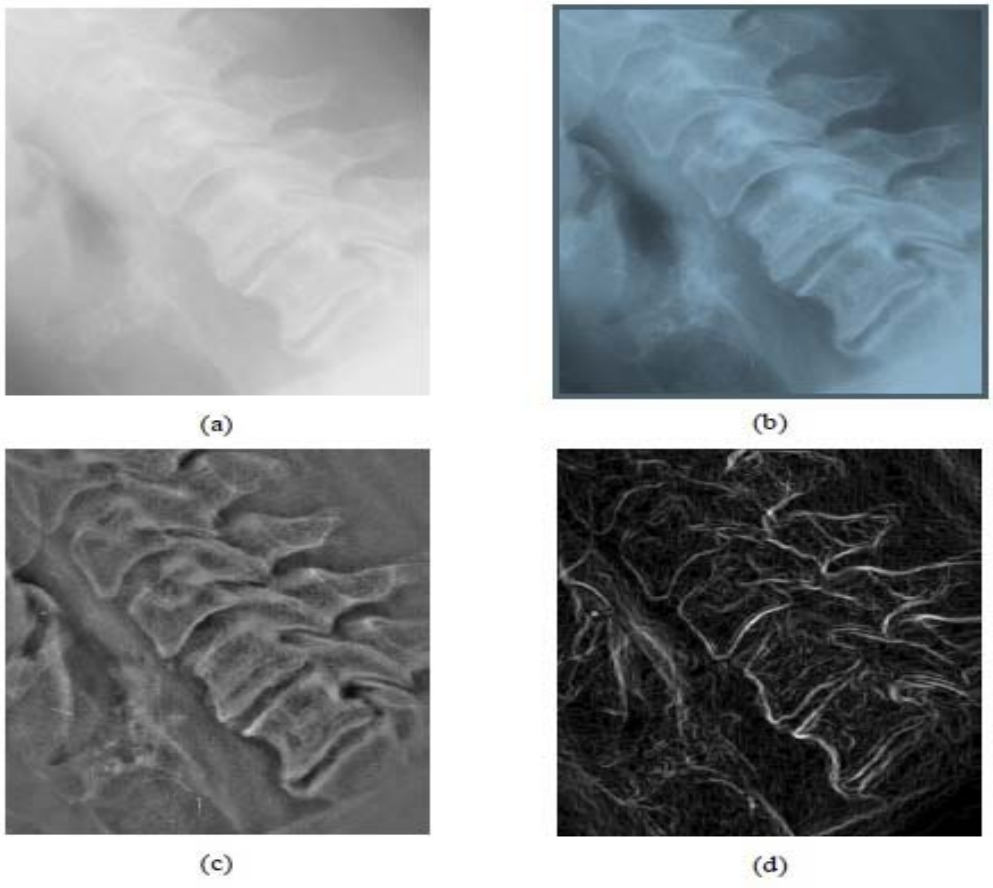

Figure (2-7): (a) A section of original X-ray image of cervical vertebra. (b) Enhanced image after adaptive histogram equalization, (c) Enhanced image after adaptive histogram equalization and unsharp masking, (d) Enhanced image after applying 3rd Derivative of Gaussian separable steerable filters ($\mu = 0.09, \sigma = 1.5$). (Cheng, 2006).

2.10.1 Filters:

Any material interposed between the x-ray tube and the film will reduce film density; filter are no exception. However, filter are used to protect the patient, and because the filter removes relatively more soft rays would otherwise be absorbed by the patient and would not emerge as remnant radiation to darken the film. The exposure rate to the patient is reduced considerably, but there is only a slight reduction in film density. (Lehmann et al., 1999).

2.10.2 Contrast:

Radiographic contrast may be defined as a variation in density. This definition tells us that contrast is a difference in densities and that at least two density levels must be present. Density and contrast are discussed as if they were separate properties, but the definition of contrast reminds us of the interdependence of the two. Although it is possible to have density without contrast, it is not possible to have contrast without density. The factors affecting contrast are: subject contrast, kilo voltage, contrast media, type of film, intensifying screens, fog, grid and beam-limiting devices, film processing, filters and x-ray beam angle. Contrast generally refers to the difference in luminance or grey level values in an image and is an important characteristic. It can be defined as the ratio of the maximum intensity to the minimum intensity over an image. Contrast ratio has a strong bearing on the resolving power and detectability of an image. Larger this ratio, more easy it is to interpret the image. Satellite images lack adequate contrast and require contrast improvement. (Lehmann et al., 1999).

2.10.3 Contrast enhancement:

One of the very first image processing issues is the contrast enhancement. The acquired image does not usually present the desired object contrast. The improvement of contrast is absolutely needed as the organ shape,

boundaries and internal functionality can be better depicted. In addition, organ delineation can be achieved in many cases without removing the background activity. (Lehmann et al., 1999).

Byte-Scaling: The scaling process is linear with the minimum data value scaled to 0 and the maximum data value scaled to 255. The BYTSCL function can be used to perform this scaling process. If the range of the pixel values within an image is less than 0 to 255, the BYTSCL can use function to increase the range from 0 to 255. This change will increase the contrast within the image by increasing the brightness of darker regions. Keywords to the BYTSCL function also allow decreasing contrast by setting the highest value of the image to less than 255.

HIST_EQUAL: used to perform basic histogram equalization within IDL. Unlike histogram equalization methods performed on color tables, the HIST_EQUAL function results in a modified image, which has a different histogram than the original image. The resulting image shows more variations (increased contrast) within uniform areas than the original image. Adaptive histogram equalization involves applying equalization based on the local region surrounding each pixel. Each pixel is mapped to intensity proportional to its rank within the surrounding neighborhood. This type of equalization also tends to reduce the disparity between peaks and valleys within the image's histogram. ADAPT_HIST_EQUAL function used to perform the adaptive histogram equalization process within IDL. Like the HIST_EQUAL function, the ADAPT_HIST_EQUAL function results in a modified image, which has a different histogram than the original image. (Lehmann et al., 1999).

Smoothing an Image: Smoothing is often used to reduce noise within an image or to produce a less pixilated image. Most smoothing methods are based on low pass filters. Smoothing is also usually based on a single

value representing the image, such as the average value of the image or the middle (median) value. (Lehmann et al., 1999).

Sharpening an Image: Sharpening an image increases the contrast between bright and dark regions to bring out features. The sharpening process is basically the application of a high pass filter to an image. The following array is a kernel for a common high pass filter used to sharpen an image; filters can be applied to images in IDL with the CONVOL function. (Lehmann et al., 1999).

Image interpolation: Interpolation is a topic that has been widely used in image processing. It constitutes of the most common procedure in order to resample an image, to generate a new image based on the pattern of an existing one. Moreover, re-sampling is usually required in medical image processing in order to enhance the image quality or to retrieve lost information after compression of an image. (Lehmann et al., 1999).

The interpolation process, these options include the resizing of an image according to a defined scaling factor, the choice of the interpolation type and the choice of low pass filter. The general command that performs image resizing is imresize. However, the way that the whole function has to be written depends heavily on the characteristics of the new image. The size of the image can be defined as a scaling factor of the existing image or by exact number of pixels in rows and columns. Spatial interpolation techniques here the pixel values of unknown pixels are estimated using the pixel values of known neigh bouring pixels. Suppose the image above is zoomed again and suppose that this time the known pixels are distributed to the corners of the zoomed image (Lyra, et al, 2011).

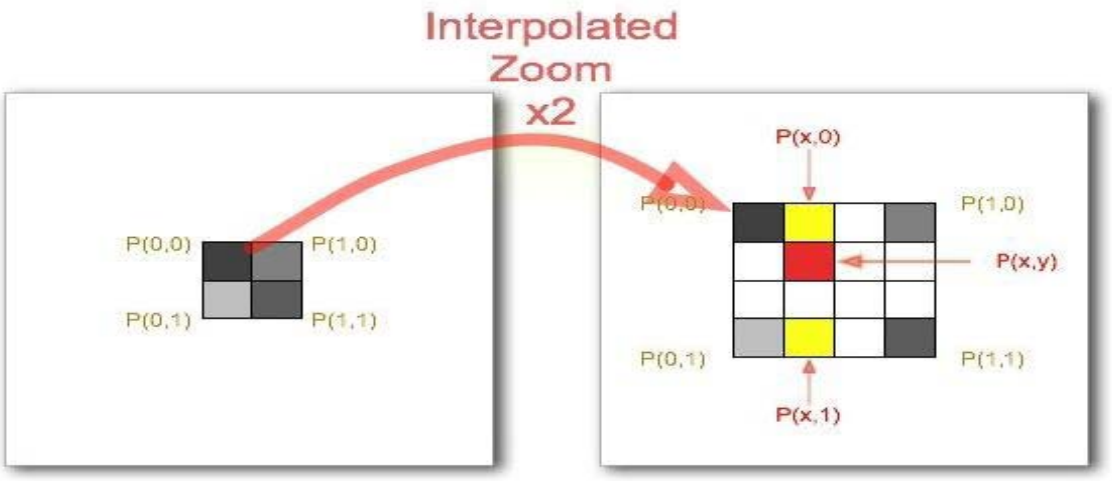

Figure (2.8): Interpolation applied to zooming an image by a factor of two (Maher et al, 2006).

Image segmentation: The image segmentation describes the process through which an image is divided into constituent parts, regions or objects in order to isolate and study separately areas of special interest. This process assists in detecting critical parts of a nuclear medicine image that are not easily displayed in the original image. The process of segmentation has been developed based on lots of intentions such as delineating an object in a gradient image, defining the region of interest or separating convex components in distance-transformed images. Attention should be spent in order to avoid 'over segmentation' or 'under-segmentation'. In nuclear medicine, segmentation techniques are used to detect the extent of a tissue, an organ, a tumor inside an image, the boundaries of structures in cases that these are ambiguous and the areas that radiopharmaceutical concentrate in a greater extent. Thus, the segmentation process serves in assisting the implementation of other procedures; in other words, it constitutes the fundamental step of some basic medical image processing. There are two ways of image segmentation: based on the discontinuities and based on the similarities of structures inside an image. In nuclear medicine images, the discontinuity

segmentation type finds more applications. This type depends on the detection of discontinuities or else, edges, inside the image using a threshold. The implementation of threshold helps in two main issues: the removal of unnecessary information from the image (background activity),the appearance of details not easily detected. The edge detection uses the command edge. In addition, a threshold is applied in order to detect edges above defined grey-scale intensity. Also, different methods of edge detection can be applied according to the filter each of them utilizes. The most useful methods in nuclear medicine are the 'Sobel', 'Prewitt', 'Roberts', 'Canny' as well as 'Laplacian of Gaussian'. It is noted that the image is immediately transformed into a binary image and edges are detected. In nuclear medicine, the methods that find wide application are the sorbel, prewitt and canny another application of segmentation in nuclear medicine is the use of gradient magnitude. The original image is loaded then the edge detection method of sobel is applied in accordance with a gradient magnitude which gives higher regions with higher grey-scale intensity. (Zitova & Flusser, 2003).

Image registration: Is used for aligning two images of the same object into a common coordinate system presenting the fused image, The images can be acquired from different angles, at different times, by different or same modalities. A typical example is the combination of SPECT and CT images or PET and CT, Image registration is used mainly for two reasons: i) to obtain enhanced information and details from the image for more accurate diagnosis or therapy to compare patient's data. (Zitova & Flusser, 2003).

IDL can be used in order to perform such a process. The whole procedure shall follow a specific order. The first step of the procedure includes the image acquisition and enhancements in brightness and contrast. The next step includes the foundation of a spatial transformation between the two

images. The final step in image registration is the overlapping of the two images allowing a suitable level of transparency. A new image is created containing information from both pictures from which, the first has been produced (Delbeke et al., 2009).

Signal-to-Noise Ratio: In order to visualize an object in a specific image, the object must have different brightness that its surroundings. Thus, the contrast of the object (signal) must overcome the image noise. The signal-to-noise ratio (SNR) is an expression used to describe the power ratio between the signal (significant information) and the background noise. In one imaging application view, these quantities would be a fixed known activity concentration and the standard deviation of its inherently fluctuating measured values attributable to the imaging protocol Considering that the mean describes what is being measured (x) and the standard deviation represents the amount of noise and other interferences, $\sigma(N)$, one can define the SNR as demonstrated on Equation (1). (Delbeke et al., 2009).

SNR=x (N) ……...(1)

2.10.4 Histogram Modification:

Histogram has a lot of importance in image enhancement. It reflects the characteristics of image. By modifying the histogram, image characteristics can be modified. One such example is Histogram Equalization. Histogram equalization is a nonlinear stretch that redistributes pixel values so that there is approximately the same number of pixels with each value within a range. The result approximates a flat histogram. Therefore, contrast is increased at the peaks and lessened at the tails. (Raghuveer M et al, 2004).

2.11 Texture:

Texture analysis refers to the branch of imaging science that is concerned with the description of characteristic image properties by textural features. However, there is no universally agreed-upon definition of what image texture is and in general different researchers use different definitions depending upon the particular area of application. (Nailon, 2010).

Texture is defined as the spatial variation of pixel intensities, which is a definition that is widely used and accepted in the field. The main image processing disciplines in which texture analysis techniques are used are classification, segmentation and synthesis. In image classification the goal is to classify different images or image regions into distinct groups. Texture analysis methods are well suited to this because they provide unique information on the texture, or spatial variation of pixels, of the region where they are applied. In image segmentation problems the aim is to establish boundaries between different image regions. By applying texture analysis methods to an image, and determining the precise location where texture feature values change significantly, boundaries between regions can be established. Synthesising image texture is important in three-dimensional (3D) computer graphics applications where the goal is to generate highly complex and realistic looking surfaces. Fractals have proven to be a mathematically elegant means of generating textured surfaces through the iteration of concise equations. (Nailon, 2010).

Conversely the ability to accurately represent a textured surface by a concise set of fractal equations has led to significant advances in image compression applications using fractal methods. Although there is no strict definition of the image texture, it is easily perceived by humans and is believed to be a rich source of visual information about the nature and

three dimensional shape of physical objects. Generally speaking, textures are complex visual patterns composed of entities, or sub patterns, that have characteristic brightness, color, slope, size, etc. Thus texture can be regarded as a similarity grouping in an image. (William, 2010).

The local sub pattern properties give rise to the perceived lightness, uniformity, density, roughness, regularity, linearity, frequency, phase, directionality, coarseness, randomness, fineness, smoothness, granulation, etc., of the texture as a whole. There are four major issues in texture analysis:

Feature extraction: to compute a characteristic of a digital image able to numerically describe its texture properties;

Texture discrimination: to partition a textured image into regions, each corresponding to a perceptually homogeneous texture (leads to image segmentation);

Texture classification: to determine to which of a finite number of physically defined classes (such as normal and abnormal tissue) a homogeneous texture region belongs;

Shape from texture: to reconstruct 3D surface geometry from texture information. Feature extraction is the first stage of image texture analysis. Results obtained from this stage are used for texture discrimination, texture classification or object shape determination. This review is confined mainly to feature extraction and texture discrimination techniques. Most common texture models will be shortly discussed as well. (William, 2010).

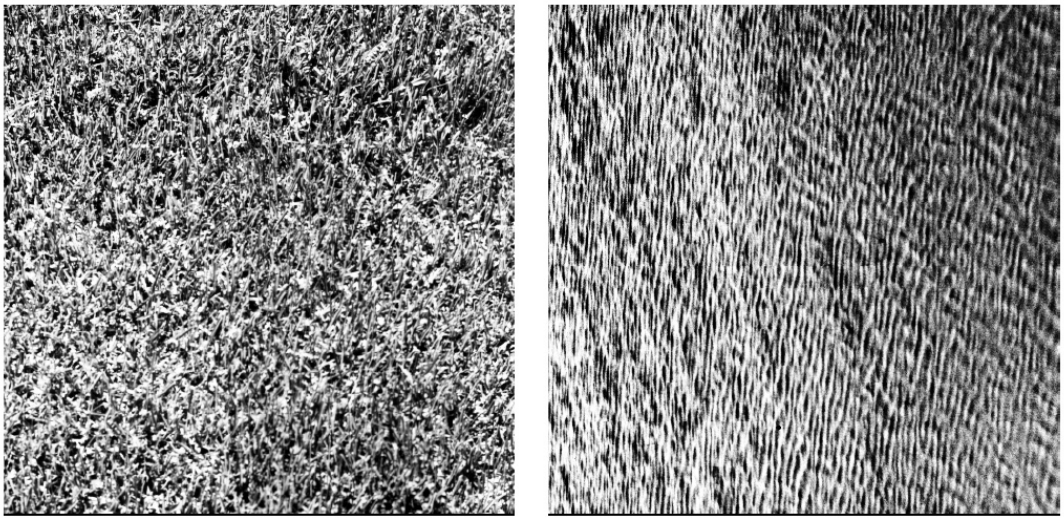

Fig (2-9): Digital images of two visibly different textured regions extracted from the Brodatz texture database (Brodatz, 1966). Left, image of grass (1.2.01, D9 H.E.). Right, image of water (1.2.08, D38 H.E.) (Weber, 2004).(Coggins, 1982).

2.12 IDL in image processing:

IDL (Interactive Data Language) is a high-level programming language that contains an extensive library of image processing and analysis routines. With IDL, you can quickly access image data and begin investigating the best way to extract useful information. IDL supports a number of different techniques for communicating with the operating system and programs written in other languages. These methods are described, in brief, below. Options are presented in approximate order of increasing complexity. We recommend that you favor the simpler options at the head of this list over the more complex ones that follow if they are capable of solving your problem. It can be difficult to choose the best option there is a certain amount of overlap between their abilities. We highlight the advantages and disadvantages of each method as well as make recommendations to help you decide which approach to take. By comparing this list with the requirements of the problem you are trying to

solve, you should be able to quickly determine the best solution. (Founder,2004).

IDL, a significant product of Research Systems Inc., is an ideal software for interactive analysis and visualization of 2D/3D scientific data. It is a powerful array-oriented interpreted language, which combines all of the tools needed for any type of project, from interactive analysis and display to large scale commercial programming projects. The outstanding advantages of IDL include: capability to analyze large scale volume data; advanced image procesing abilities; 2D/3D interactive graphics techniques; object oriented programming; OpenGL based hardware accelerated graphics; a vast library of built-in math, statistics, image analysis, information processing routines; flexible input/output facilities; multi-platform graphical user interface (GUI) widgets and preferable portability. Researchers, developers, and engineers at myriad commercial corporations, governments organizations and academic institutions (e.g., Mars Exploration Team, NASA, Los Alamos National Lab's Biophysics Group) use IDL to bring products to market and make discoveries less expensively and in less time. As a result of the advantages of IDL mentioned above, it is decided to program in IDL, alternative to programming in C, C++, FORTRAN or MATLAB, to design and implement medical images visualization toolbox. The architecture of this article is as following: first the characteristics and advantages of IDL are introduced; secondly the several kernel programming techniques are explained, including object oriented programming, graphics system, graphical user interface and IDL virtual machine; then the experimental results are illustrated and finally the functions and advantages of our toolbox are concluded. (Founder,2004).

2.13 Previous of Studies:

In reviewing of literature in locally and internationally there are some published studies regarding the enhancement of cervical x-ray by many researchers who they are mentioned below:

Raihan Firoz et al (2015), they enhanced medical images using morphological transformation; Medical imaging includes different modalities and processes to visualize the interior of human body for diagnostic and treatment purpose. However, one of the most common degradations in medical images is their poor contrast quality and noise. The existence of several objects and the close proximity of adjacent pixels values make the diagnostic process a daunting task. The idea of image enhancement techniques is to improve the quality of an image. In this study, morphological transform operation is carried out on medical images to enhance the contrast and quality. A disk shaped mask is used in Top-Hat and Bottom-Hat transform and this mask plays a vital role in the operation. Different types and sizes of medical images need different masks so that they can be successfully enhanced. The method shown in this study takes a mask of an arbitrary size and keeps changing its size until an optimum enhanced image is obtained from the transformation operation. The enhancement is achieved via an iterative exfoliation process. The results indicate that this method improves the contrast of medical images and can help with better diagnosis.

B.Vasumathi and Thangam (2015), played a vital role in the analysis and interpretation of remotely sensed data. Especially data obtained from Satellite Remote Sensing, which is in the digital form, can best be utilized with the help of digital image processing. Image enhancement and information extraction are two important components of digital image

processing. Image enhancement techniques help in improving the visibility of any portion or feature of the image suppressing the information in other portions or features. Information extraction techniques help in obtaining the statistical information about any particular feature or portion of the image. These techniques are discussed in detail and illustrated in this article.

Dung et al (2014) Implemented Shock Filter for Digital X-Ray Image Processing X-ray image might be corrupted by noise or blurring because of signal transmission or the bad X-ray lens. This paper presents a two-stage shock filter based on Partial Differential Equations (PDE) to restore noisy blurred X-ray image. Shock filters are popular morphological methods. They are used for noise removal, edge enhancement and image segmentation. Our experimental results show that the performances of shock filter are excellent in X-ray image. The peak signal-to-noise ratio (PSNR) values are 38 dB at least in restoring the noisy X-ray image. The sharpness of image's edges increase in enhancing the blurred X-ray image. Furthermore, this paper proposes VLSI architecture for accelerating the high-definition (HD) X-ray image (944 p) process. This paper implements the architecture in FPGA. The hardware cost is low because the computation of shock filter is low complex. To achieve the real-time processing specification, this paper uses a 5-series shock filter architecture to implement computation of HD X-ray image. This paper demonstrates a 944 p, 43.1-fps solution on 100 MHz with 133 k gate counts in Design Compiler, and with 2904 logic elements in FPGA.

Duan et al (2013) applied the classical TV (Total Variation) model to gray texture image denoising and inpainting previously based on the non-local operators, but such model cannot be directly used to color texture

image inpainting due to coupling of different image layers in color images. In order to solve the inpainting problem for color texture images effectively, we propose a non local CTV (Color Total Variation) model. Technically, the proposed model is an extension of local TV model for gray images but we take account of the coupling of different layers in color images and make use of concepts of the non-local operators. As the coupling of different layers for color images in the proposed model will in- crease computational complexity, we also design a fast Split Bregman algorithm. Finally, some numerical experiments are conducted to validate the performance of the proposed model and its algorithm.

Ogawa et al (2013) they removed the shadow of cervical vertebrae from dental panoramic x-ray images with a tomosynthesis method and improve the contrast of details in both the teeth and jaw bones. To measure the shift-amount at each angular position that was required for reconstruction of panoramic x-ray images of the dental arch, strip images of a calibration phantom were acquired. Then, a shift-amount table was prepared from these images, and the other shift- amount table, which was used to reconstruct a panoramic image of the cervical vertebrae, was prepared by inverting the curve of the shift-amount table upside down. Using these two tables, images focused on the dental arch and cervical vertebrae of a patient were made with the original strip data of the patient. The shadow of the cervical vertebrae appearing on the image focused on the dental arch was removed using the two above-mentioned images and blurring functions defined at two focusing geometries. The validity of the proposed method was evaluated with clinically acquired data of two patients. The shadow of the cervical vertebrae was successfully eliminated, and the contrast of the front teeth and detailed structures of the jaw bones was improved. The results of the experiments showed that

our pro-posed method was significantly effective in removing the shadow of the cervical vertebrae from conventional panoramic x-ray images.

An Efficient Contrast Enhancement of Medical X-Ray Images –Adaptive Region Growing Approach , In digital image processing Medical Imaging is one of the most significant application areas. For visualizing and extracting more details from the given image processing of medical images is much more supportive. Several techniques are existing nowadays for enhancing the quality of medical image. Contrast Enhancement is one of the most functional methods for the enhancement of medical images. Various contrast enhancement techniques are in practice, some are as follows: Linear Stretch, Histogram Equalization, Convolution mask enhancement, Region based enhancement, Adaptive enhancement is already available. Based on characteristics of image choices can be done. On comparing their approach with the existing popular approaches of adaptive enhancement and linear stretching, it has been concluded that the proposed technique is giving much better results than the existing ones. Further, the technique is seed dependent so selection of seed is very important in this algorithm. A seed chosen in darker regions will give better results than the seed chosen in brighter region, because it is assumed that user will require enhancing the darker portions of the image. Furthermore, zooming window and edge growing method is used to visualize the edges more precisely which gives an added advantage is to doctors for better perception of X-ray (Krishna and Khanaa 2013).

Hari and Mantosh (2012), used a New Image Denoising Scheme Using Soft-Thresholding, The VisuShrink is one of the important image denoising methods. It however does not provide good quality of image

due to removing too many coefficients especially using soft-thresholding technique. This paper proposes a new image denoising scheme using wavelet transformation, they modify the coefficients using soft-thresholding method to enhance the visual quality of noisy image. The experimental results show that our proposed scheme has bet-ter performance than the VisuShrink in terms of peak signal-to-noise ratio (PSNR) *i.e.*, visual quality of the image.

Lavania and Kumar (2011) presented two methods of Image enhancement that improves the visual quality of image. In this paper, the authors compare two histogram techniques: Histogram Equalization and Histogram Specification. Histogram Equalization is a technique that generates a gray map which changes the histogram of an image and redistributing all pixels values to be as close as possible to a user – specified desired histogram. Histogram specification is a technique to enhance certain regions of an image. A measure of enhancement (EME) based on contrastrespect to transform is used as a tool for evaluating the performance of the enhancement techniques. The author implement and analyze the result of these two approaches based on EME using Image Processing Toolbox (IPT) and their performance evaluated on various images.

Wei et al (2011) enhanced X-ray image using algorithm based on AH (adaptive histogram) and MSR (Multi-scale Retinex) algorithm is proposed in this paper for the industrial X-ray image, which contrast is low, and the detail features is poor. Firstly, the contrast limited adaptive histogram equalization and neighborhood algorithm is used for the image. Then the mapping is built between the image and the detail scales by the enhance function ratio rules, which is adjusted by the local contracting

information. Finally, according the enhance function radios, the reconstructed image is rebuild. Compared with other image enhancement algorithms, experimental results show that our algorithm can improve the global image effectively, moreover it overcomes the visible artifacts of X-ray image. Therefore, the x-ray image becomes clearer, and a better perceptual image is acquired for the image feature recognizing and matching.

Mahendran and Baboo (2011) Enhanced Tibia Fracture Detection Tool Using Image Processing and Classification Fusion Techniques in X-Ray Images; in their study Automatic detection of fractures from x-ray images is considered as an important process in medical image analysis by both orthopaedic and radiologic point of view. This paper proposes a fusion-classification technique for automatic fracture detection from long bones, in particular the leg bones (Tibia bones). The proposed system has four steps, namely, preprocessing, segmentation, feature extraction and bone detect ion, which uses an amalgamation of image processing techniques for successful detection of fractures. Three classifiers, Feed Forward Back Propagation Neural Networks (BPNN), Support Vector Machine Classifiers (SVM) and Naïve Bayes Classifiers (NB) are used during fusion classification. The results from various experiments prove that the proposed system is shows significant improvement in terms of detection rate and speed of classification.

Ahmad and Hanung (2009), applied retinal vasculature enhancement using independent component analysis, Retinal vasculature is a network of vessels in the retinal layer. In ophthalmology, information of retinal vasculature in analyzing fundus images is important for early detection of diseases related to the retina, e.g. diabetic retinopathy. However, in

fundus images the contrast between retinal vasculature and the background is very low. As a result, analyzing or visualizing tiny retinal vasculature is difficult. There- fore, enhancement of retinal vasculature in digital fundus image is important to provide better visualization of retinal blood vessels as well as to increase accuracy of retinal vasculature segmentation. Fluorescein angiogram overcomes this imaging problem but it is an invasive procedure that leads to other physiological problems. In this research work, the low contrast problem of retinal fundus images obtained from fundus camera is addressed. We develop a fundus image model based on probability distribution function of melanin, hemoglobin and macular pigment to represent melanin, retinal vasculature and macular region, respectively. We determine retinal pigments makeup, namely macular pigment, melanin and hemoglobin using independent component analysis. Independent component image due to hemoglobin obtained is used since it exhibits higher contrast retinal vasculature. Contrast of retinal vasculature from independent component image due to hemoglobin is compared to those from other enhancement methods. Results show that this approach outperforms other non-invasive enhancement methods, such as contrast stretching, histogram equalization and CLAHE and can be beneficial for retinal vasculature segmentation. Contrast enhancement factor up to 2.62 for a digital retinal fundus image model is achieved. This improvement in contrast reduces the need of applying contrasting agent on patients.

CHAPTER THREE

Chapter Three
Materials and Methods

3.1 Materials:

Personal Computer (PC), IDL program, X-ray machine.

The study executed using X-ray machine; This table show the feature of the X-ray machine:

Table (3-1): show the feature of the X-ray machine:

Name of hospital	Company	KV Range	mAs Range	Serial Number	Tube rotation	Table Rotation
Antalya Medical Center	ALLENGERS	65-125	300 - 500	2K101150180-X	360	180 degree

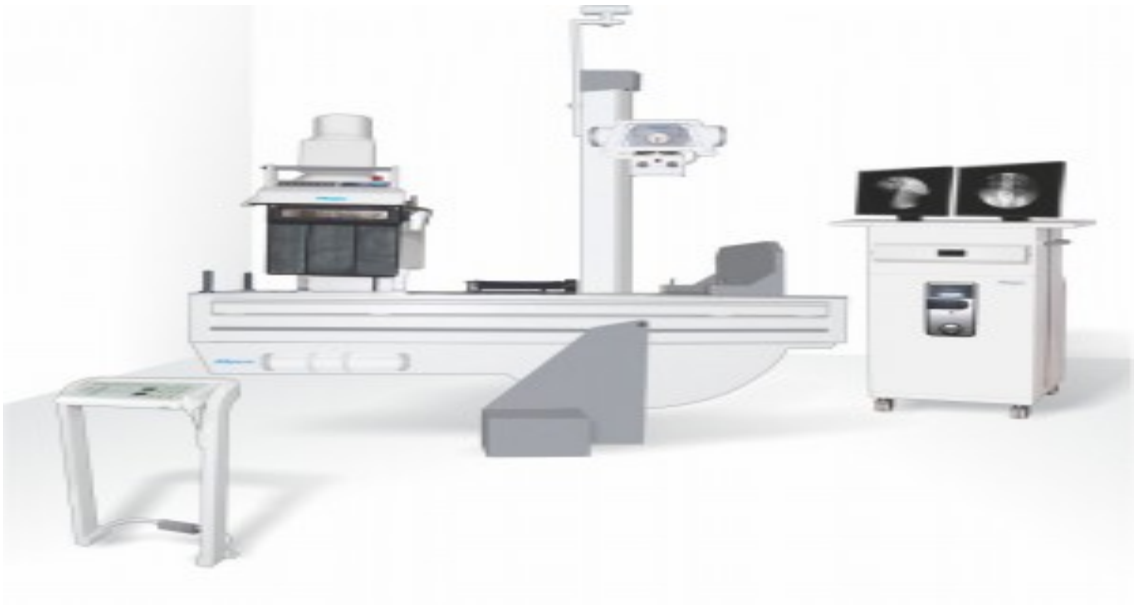

Figure (3-1): Demonstrated X-Ray Machine Line Frequency

3.2 Methods:

3.2.1 Place and duration of the Study:

This study conducted in Sudan University - College of Radiology during the period from May 2017 to October 2017.

3.2.2 Study Population:

Total of 50 patients examined cervical x-ray were from both gender male and females and they were adults, the images are taken for different reasons.

3.2.3 Study design:

This is an analytical study where the data collected from the radiograph before enhancement were compared to the data collected after enhancement.

3.2.4 Sampling and type:

Total of 50 patients examined Cervical x-ray in diagnostic department in Antalya Medical Center, the radiograph which are taken was CR radiograph.

3.3 Method of data Collection:

The total of 50 patients have underwent to cervical x-ray it will be collected in Antalya Medical Center. Then enhancement of the data by using image processing technique. The cervical spine radiograph were read by IDL program where a region chosen in a low intensity area by clicking on that region then repeat the same process in a high intensity area located nearby the first region. Then noise, signal, signal to noise ratio and contrast were calculated in both region. After that the

radiograph enhanced using histogram equalization function and the same quality were collected again and after applying filtering using median filter the same process repeated.

3.4 Method of data presentation:

After that Cervical x-ray radiograph were stored in computer disk were viewed by the Radiant, Ant DICOM viewer in computer to selected the axial radiograph that suit the criteria of research population then uploaded into the computer based software Interactive Data Language (IDL) where the DICOM radiograph converted to TIFF format to suit IDL platform in order to preserve the quality of the radiograph.

3.5 Methods of data analysis:

The mean and standard deviation of the noise, signal, signal to noise ratio and contrast calculated data from the low and high intensity area, and scatter plot shows the linear relationship between these quantities before and after enhancement were displayed to fined the coefficient of improvement after enhancement.

CHAPTER FOUR

Chapter four
The results

The result of this study consisted of: signal before and after enhancement, noise before and after enhancement, signal to noise ratio before and after enhancement, contrast before and after enhancement.

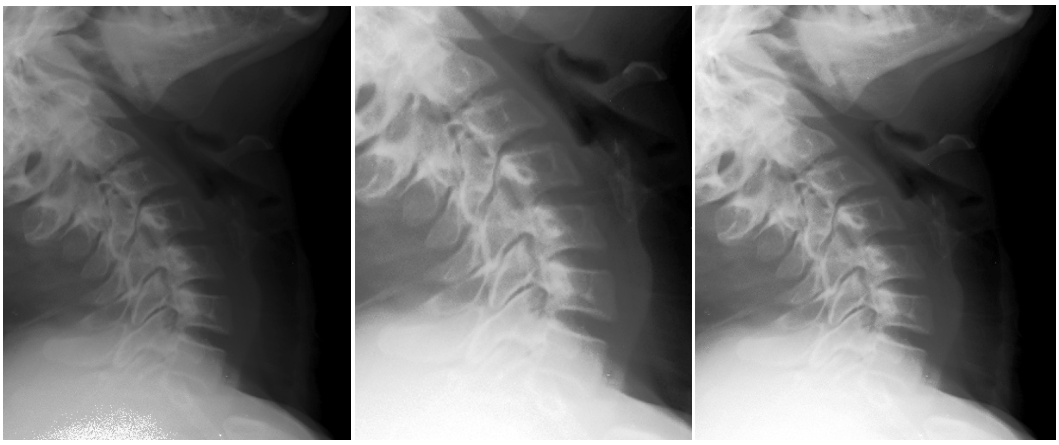

(A) Normal (B) Histogram Equalization (C) Enhanced

Figure (4-1): Demonstrated original radiograph for cervical spine (A) the original radiograph (B) showed radiograph after Histogram equalization. (C) Showed an radiograph after median filter smoothing.

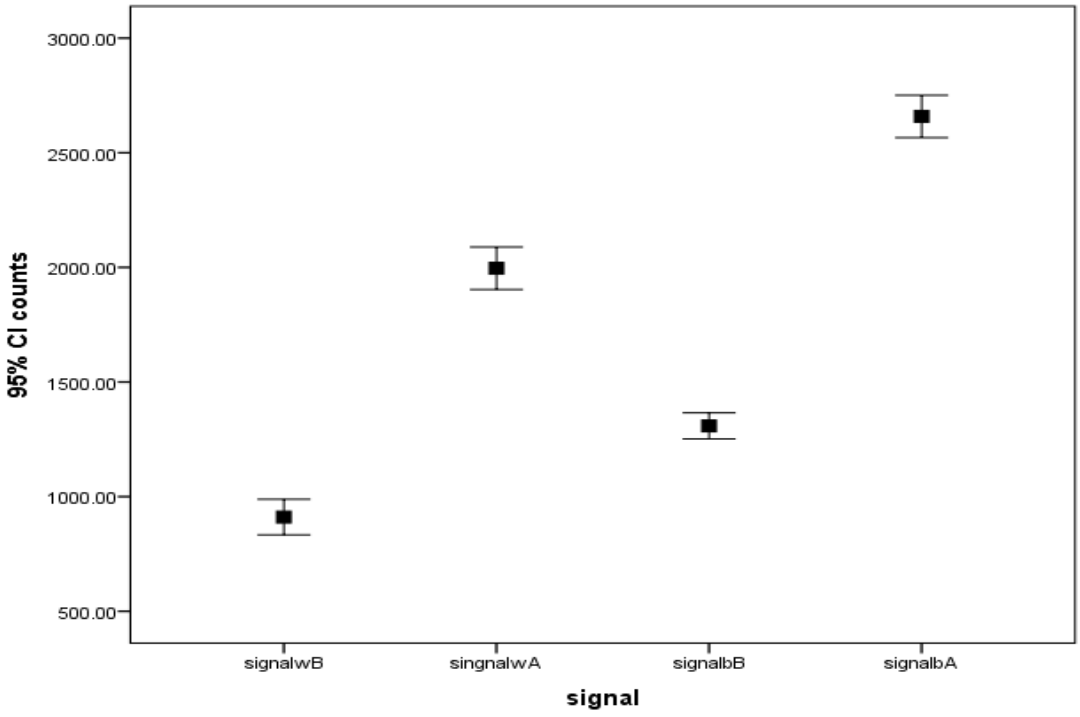

Figure (4-2): Simple error bar demonstrate the difference in signal in the white(w) and dark(b) area before(B) and after(A) enhancement

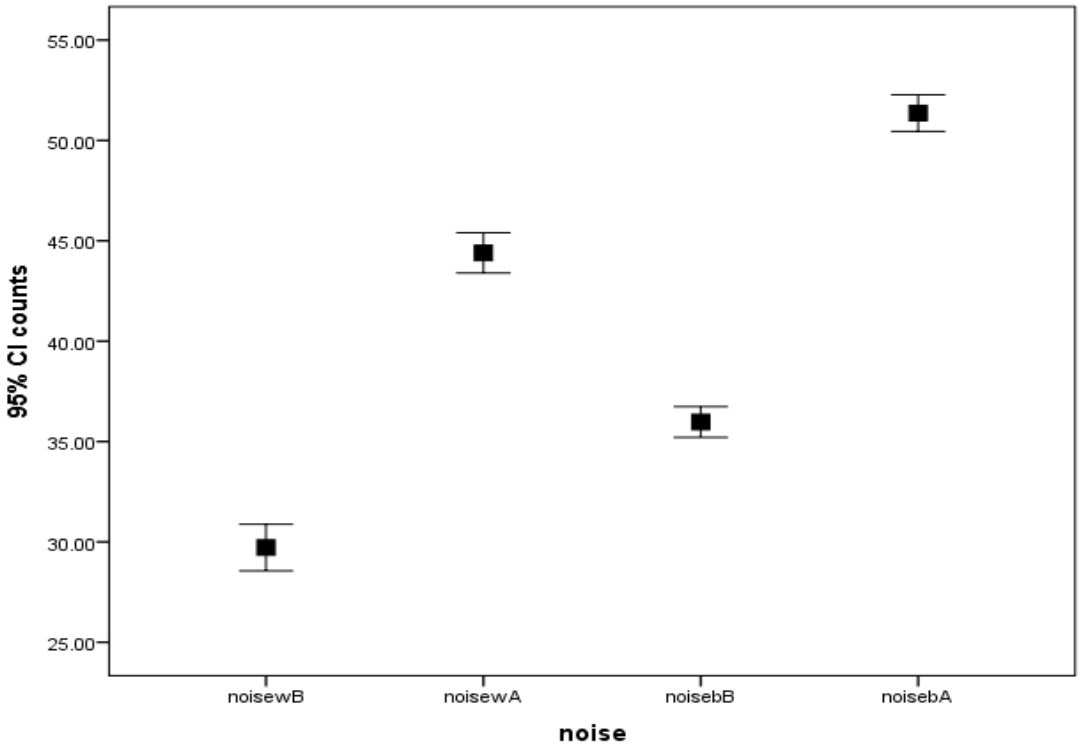

Figure (4-3): Simple error bar demonstrate the difference in noise in the white(w) and dark(b) area before(B) and after(A) enhancement

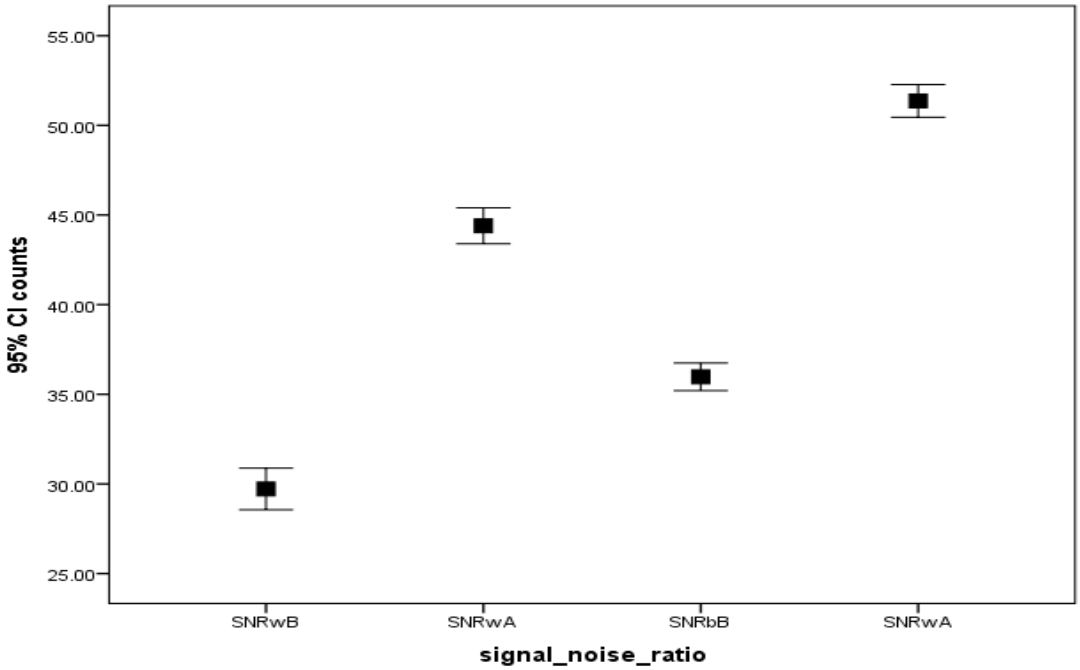

Figure (4-4): Simple error bar demonstrate the difference in signal/noise ratio before and after enhancement

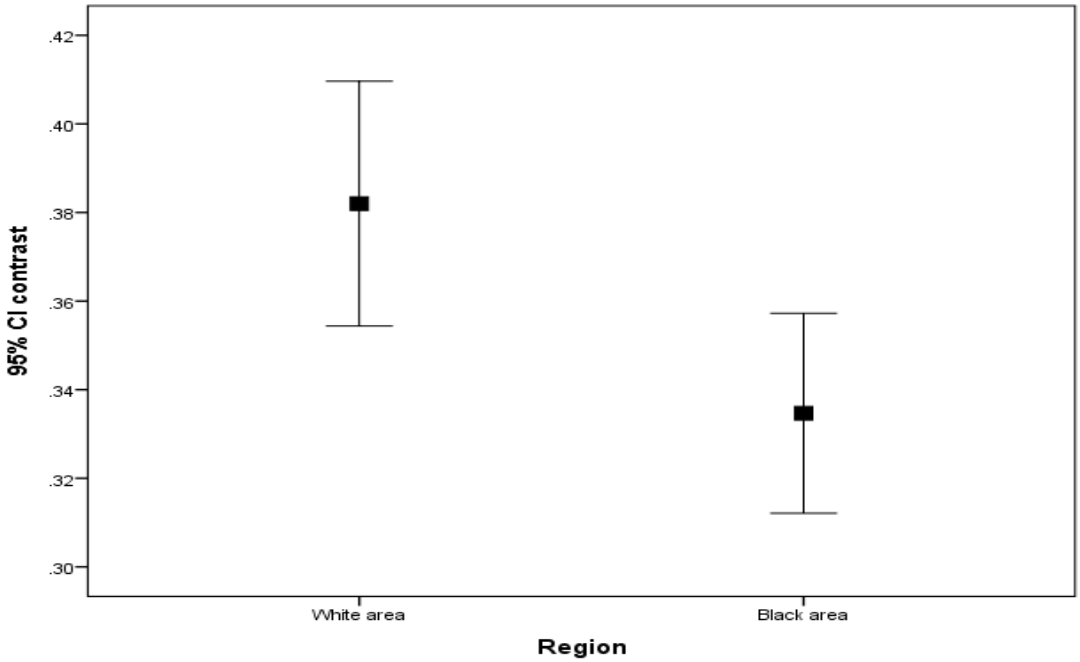

Figure (4-5): Simple error bar demonstrate the difference in contrast in white and dark area before and after enhancement

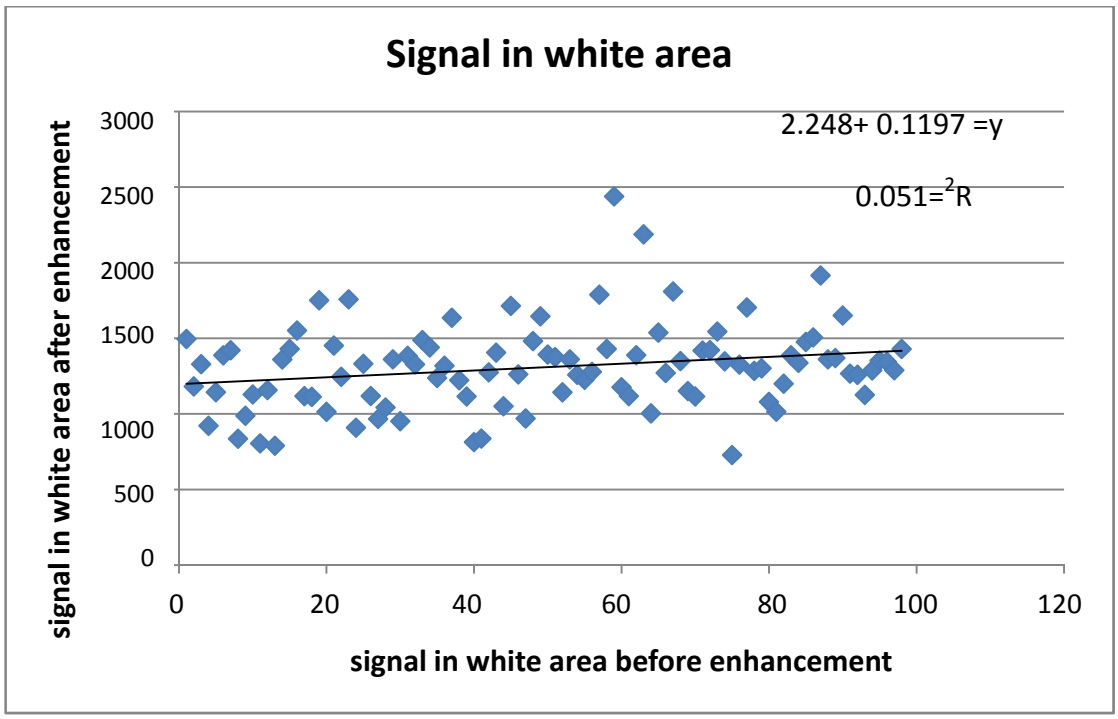

Figure (4-6): Showing the relationship between signal in white area before and after enhancement

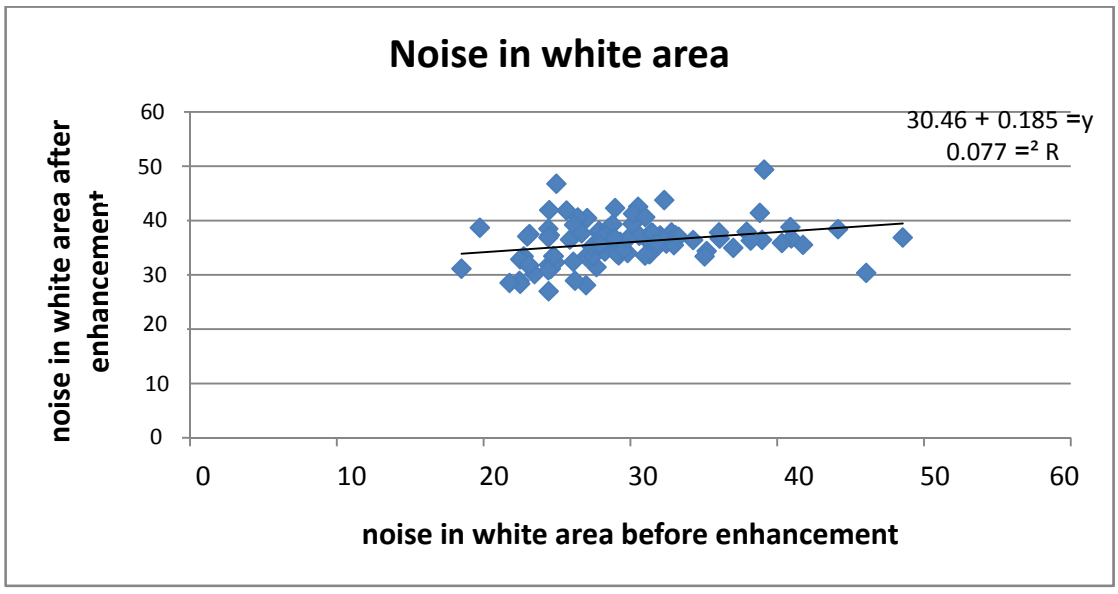

Figure (4-7): Showing the relationship between noise in white area before and after enhancement

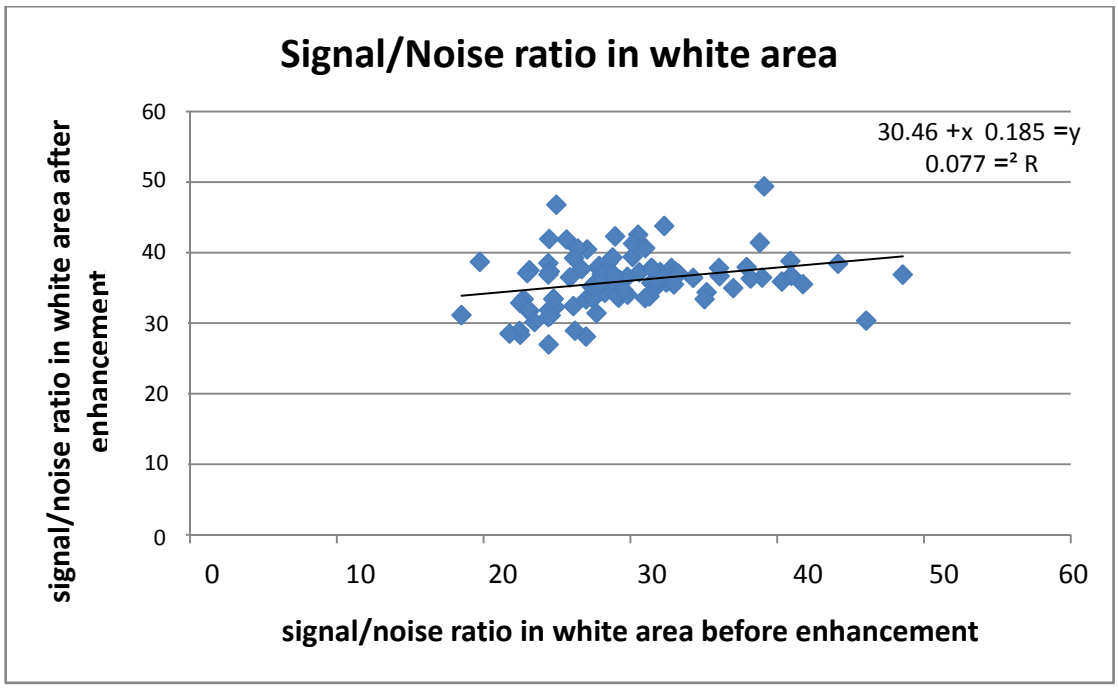

Figure (4-8): Showing the relationship between signal to noise ratio in white area before and after enhancement

Table (4-1): Shows the mean and standard deviation in White area before and after enhancement:

Item	Mean±SD before enhancement	Mean±SD after enhancement
signal	920.2±376.7	1308.6±282.3
noise	29.7±5.8	36.0±3.8
S/N ratio	29.7±5.8	36.0±3.8

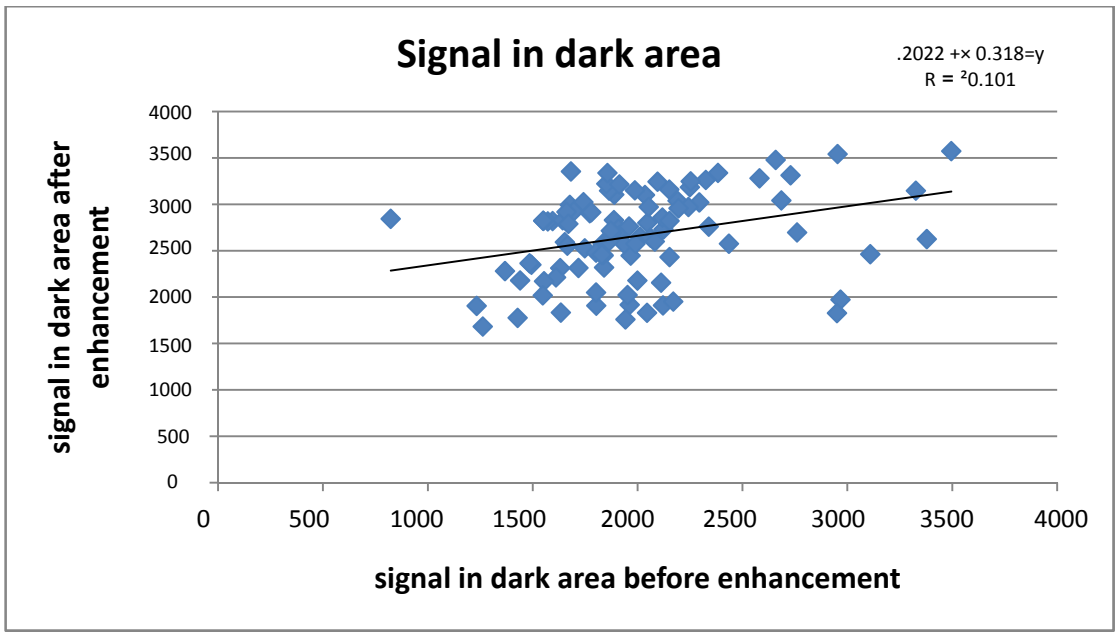

Figure (4-9): Showing the relationship between signal in dark area before and after enhancement

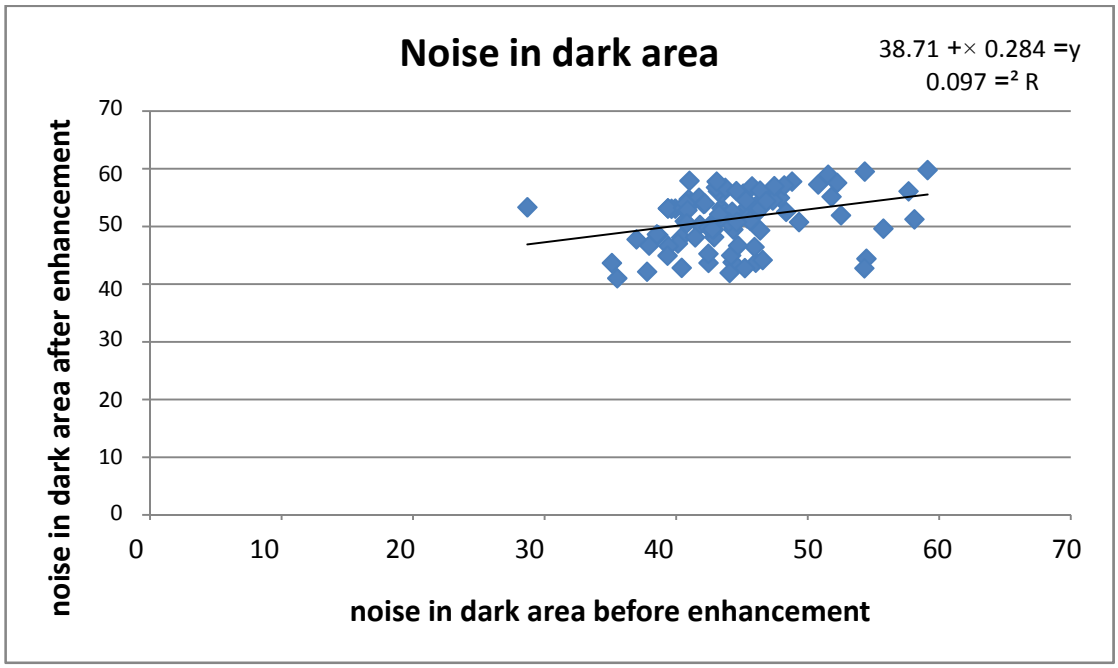

Figure (4-10): Showing the relationship between noise in dark area before and after enhancement

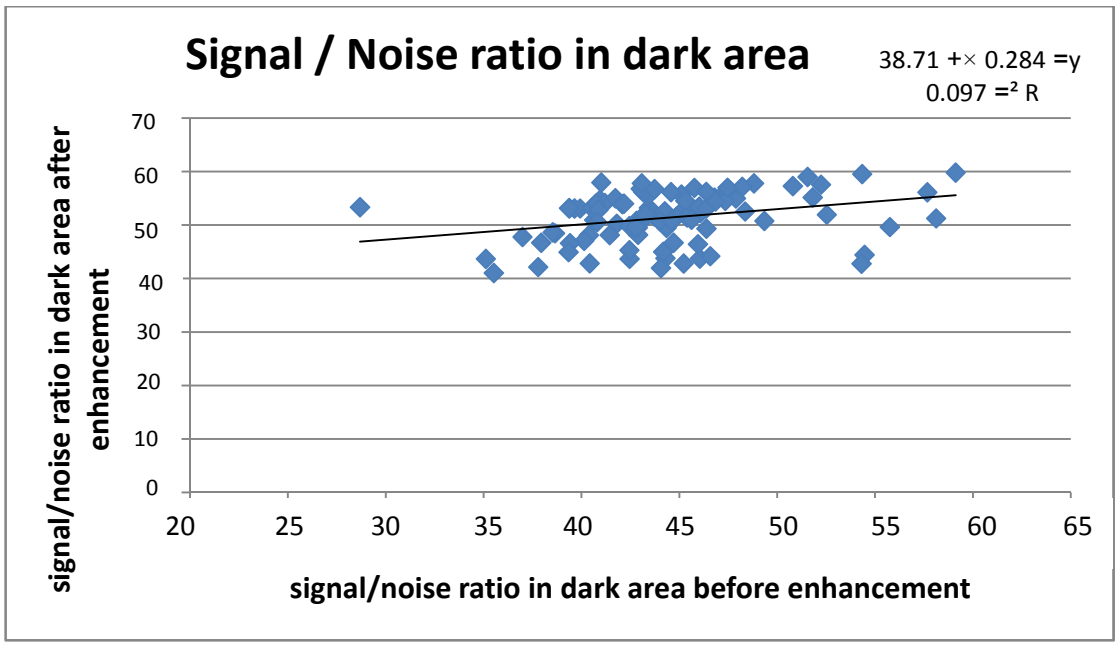

Figure (4-11): Showing the relationship between signal to noise ratio in dark area before and after enhancement

Table (4-2): Shows the mean and standard deviation in dark area before and after enhancement:

Item	Mean±SD before enhancement	Mean±SD after enhancement
signal	1996.03±461.0	2658.6±461.0
noise	44.40±5.0	51.36±4.6
S/N ratio	44.40 ±5.0	51.36±4.6

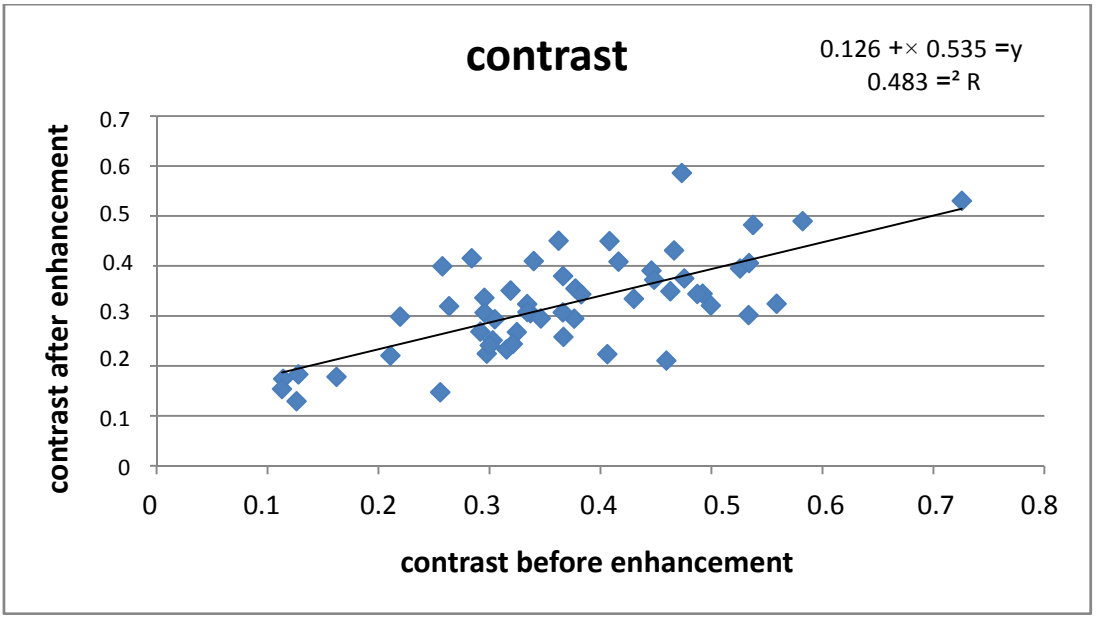

Figure (4-12): Showing the relationship between contrast before and after enhancement

Table (4-3): Shows the mean and standard for contrast before and after enhancement:

Item	mean±SD before enhancement	mean±SD after enhancement
Contrast	0.38±0.14	0.34±0.11

CHAPTER FIVE

Chapter five
Discussion, Conclusion, and Recommendation

This study was aimed to enhance cervical x-ray radiographs using image processing technique, the study was done in Antalya Medical Center-Khartoum-Sudan, and 50 cervical x-ray radiograph were processed using IDL software with details as follows: In this study data analyzed by using IDL program to enhance the contrast with in the bone and soft tissue, reduce the noise, filter the radiographs and find signal to noise ratio. The technique used for this study was histogram equalization and mean filter.

5.1 Discussion:

The result of this study as show in Figure (4-2) error bar for four classes counts classified using the signal were the feature signal classified well the four classes. In Figure (4-3) error bar for four classes counts classified using the noise were the feature noise classified well the four classes. In Figure (4-4) error bar for four classes counts classified using the signal/noise ratio were the feature SNR classified well the four classes. In Figure (4-5) error bar for four classes counts classified using the contrast were the feature contrast classified well the four classes.

In case of white area the amount of the signal before and after enhancement by histogram equalization was 920.2±376.7 and 1308.6±282.3 respectively in figure (4-6) and table (4-1), this mean the enhancement increase the amount of signal by 1 Per 2.25 for every one unit from x-axis which would be filtered before and after enhancement, starting by 1197 as enhance level threshold, when the value of the signal approached to zero before enhancement.

Also in white area the amount of the noise before and after enhancement by histogram equalization was 29.7±5.8 and 36.0±3.8 respectively in

figure (4-7) and table (4-1), this mean the enhancement increase the amount of noise by 1 Per 36.0±3.8 For every one unit from x-axis which would be filtered before and after enhancement, starting by 30.5 as enhance level threshold, when the value of the noise approached to zero before enhancement.

Show in Figure (4-8) and table (4-1) the signal to noise ratio before and after enhancement by histogram equalization was 29.7±5.8 and 36.0±3.8 respectively for white area. This mean the enhancement increase the amount of signal to noise ratio by 1 Per 0.185 count for every one unite from x-axis which would be filtered before and after enhancement, starting by 30.5 as enhance level threshold, when the value of the signal approached to zero before enhancement.

In case of dark area the amount of the signal before and after enhancement by histogram equalization was 1996.03±461.0 and 2658.6±461.0 respectively in figure (4-9) and table (4-2), this mean the enhancement increase the amount of signal by 1 Per 0.3188 for every one unit from x-axis which would be filtered before and after enhancement, starting by 2022.3 as enhance level threshold, when the value of the signal approached to zero before enhancement.

Also in dark area the amount of the noise before and after enhancement by histogram equalization was 44.40±5.0 and 51.36±4.6 respectively in figure (4-10) and table (4-2), this mean the enhancement increase the amount of noise by 1 Per 0.2848 For every one unit from x-axis which would be filtered before and after enhancement, starting by 38.717 as enhance level threshold, when the value of the signal approached to zero before enhancement.

Show in Figure (4-11) and table (4-2) the signal to noise ratio before and after enhancement by histogram equalization was 44.40 ± 5.0 and 51.36 ± 4.6 respectively for dark area. This mean the enhancement increase the amount of signal to noise ratio by 1 Per 0.2848 count for every one unite from x-axis which would be filtered before and after enhancement, starting by 38.717 as enhance level threshold, when the value of the signal approached to zero before enhancement.

The amount of the contrast before and after enhancement by histogram equalization was 0.38 ± 0.14 and 0.34 ± 0.1 respectively in figure (4-12) and table (4-3). This mean the enhancement increase the amount of the contrast by 1 per 0.5352 for every 1 unit from x-axis which would be filtered before and after enhancement, starting by 0.1261 as enhance level threshold, when the value of the signal approached to zero before enhancement.

The result of this study was agreed to (Dung et al, 2014), they were used mean filter and after applied it to the radiographs, it showed that there was significant reduction in noise, and they were obtained for the similar results as mentioned above. In addition the results of (Krishna and Khanaa, 2013) and (Raihan Firoz et al 2015) showed that the histogram equalization has a good ability to produce an radiograph with high contrast (i.e) increase the visibility of the hidden region like edge and the small structures, as well as to composite the radiograph brightness and produce more sensible view.

5.2 Conclusion:

The main objective of this study was to enhance of cervical spine radiographs using image processing technique where 100 cervical spine radiographs were used, in conclusion the results of this study proved that the cervical spine radiographs quality improved as a result of enhancement where the signal to noise ratio was better after enhancement although noises was increased as a result of enhancement but the increases were very limited, as well as the used radiograph were digital one where noises were low and enhancement will starch the intensity over low intensity area and hence increase the dynamic range of the gray scale for better perception. And IDL program techniques such as histogram equalization which was used to enhanced the contrast of the radiograph in the presence of the noise, and filtering the radiograph using mean filter which were performed to reduce the noise in cervical x-ray radiographs cause the noise reduced the quality of the radiograph and visibility of the details. The result show efficiency of these techniques to improve and boost the quality of the radiographs in terms of contrast, the contrast was significantly increased and it was the mean before enhancement 0.38 and it became after enhancement 0.34.

5.3 Recommendation:

- The technologist should be trained to handle the radiograph electronically i.e. be able to highlight the region of interest.
- Other method of enhancement; like adaptive enhancement can be carried out in other studies to highlight ROI.
- Similar study can be done for different x-ray examination.

References

Bourne, Roger, "Image Filters" Fundamentals of Digital Imaging in Medicine, doi:10.1007/978-1-84882-087-67, 2009.

Coggins, J. M., 1982, “A Framework for Texture Analysis Based on Spatial Filtering,” Ph.D. Thesis, Computer Science Department, Michigan State University, East Lansing, Michigan.

David Stern Founder,2004, External Development Guide, 2004 Edition, Copyright © Research Systems, Inc.

Deen, H. Gordon, and Stephen J. Mcgirr, Vertebral Artery Injury Associated with Cervical Spine Fracture, Spine 17, no 2, (1992).

Delbeke, D.; Coleman, R.E.; Guiberteau M.J.; Brown, M.L.; Royal, H.D.; Siegel, B.A.; Gonzalez, R.; Woods, R., & Eddins, S.,2009, Digital Image Processing using MATLAB, second edition, Gatesmark Publishing, United States of America, ISBN 9780982085400.

Deserno, Thomas M, Biomedical image processing, Heidelberg: Springer, 2011.

Fabrizio Russo, 2002, "An Image Enhancement Technique Combining Sharpening and Noise Reduction", IEEE Transactions on Instrumentation and Measurement, vol.51, no.4, August.

H. Thierens, K. D’Herde, 2017 , Image quality evaluation in X-ray medical imaging based on Thiel embalmed human cadavers, htt://www.bing.com/cr?IG=30AF9B64465C9EA2EC01FFA37&CID.

Henry, William. "Texture Analysis Methods for Medical Image Characterization." Biomedical Imaging, 2010. Doi:10.5772/8912.

Image Processing in IDL, 2004 Edition, Copyright © Research Systems. Inc.

Jerrold T.Bushberg, J. Anthony Seibert, Edwin M. Leidholdt, JR and John M. Boone 2002, the essential physics of medical physics, 2nd edition, 2002 by Lippincott Williams & Wilkins.

Jing Cheng, X-ray image Segmentation and an Internet-based Tool for Medical Validation, university of maryland, 2006, pages (28-33).

Kieran Maher et al, 2006-08-12, Basic Physics of Nuclear Medicine, Publisher: Wikibooks , Kohima India, Ad ID: 348381999.

Laverne Tollery Gurley, William J. Callaway, Introduction to Radiologic Technology , Third edition, 1992, David T. Culverwell, page 104.

Lehmann, T.M.; G?nner, C. & Spitzer, K., November 1999, Survey: Interpolation Methods in Medical Image Processing, IEEE Transactions on Medical Imaging, Vol.18, No.11, pp. (1049-1075), ISSN S0278-0062(99)10280-5

Marco Bozzali, Maria A. Rocca, Giuseppe Iannucci, Clodoaldo Pereira, Giancarlo Comi and Massimo Filippi, Magnetization-Transfer Histogram Analysis of the Cervical Cord in Patients with Multiple Sclerosis, American Journal of Neuroradiology November 1999, 20 (10) 1803-1808.

Maria Lyra, Agapi Ploussi and Antonios Georgantzoglou, 2011, MATLAB as a Tool in Nuclear Medicine Image Processing, MATLAB - A Ubiquitous Tool for the Practical Engineer, Prof,Clara Ionescu (Ed.), InTech, ISBN: 978-953-307-907-3.

Michael Y. M. Chen, Thomas L. Pope, David J. Ott, Basic Radiology, 2nd edition, Copyright © 2011, 2004 by The McGraw-Hill Companies, Inc.

Rafael C. Gonzalez, Richard E. Woods, Digital Image Processing, Third Edition 2008 by Pearson Education, Inc. Pearson Prentice Hall, page (1-2, 9).

Rao D. V. G. N, and Chandra S. Yelleswarapu, " Optical Fourier Techniques for Medical Image Processing. "Biomedical Optics, 2006.

Rao, Raghuveer M., and Manoj K. Arora. "Overview of Image Processing." Advanced Image Processing Techniques for Remotely Sensed Hyperspectral Data, 2004, 51-85. doi:10.1007/978-3-662-05605-9_3.

Robert Fisher, Simon Perkins, Ashley Walker and Erik Wolfart 2000, Hypermedia Image Processing Reference. ISBN 0471962434.

Roger L. Easton, Jr, 2010, Fundamentals of Digital Image Processing.

Sonia O'conno, Mary M. Brooks (2007), X-radiography of textiles, dress and related objects first edition, Library of Congress Cataloguing in publication data, page 13.

Tinku Acharya, Ajoy K. Ray, 2005, Image Processing: Principles and Applications, Publisher John Wiley & Sons, USA, ISBN 10-0471745782, 13- 9780471745785.

Zitova, B. & Flusser J., June 2003, Image Registration methods: a survey Image and Vision Computing. Vol 21, pp. (977-1000).

APPENDIX

APPENDIX

Data (A): Enhancement factors from cervical x-ray radiograph:

sigw	noisew	SNw	sigb	noiseb	SNb	contbefor	sigwe	noisewe	snwe	sigbe	noisebe	snbe	contafte
390	19.7484	19.7484	823	28.688	28.688	-0.35697	1496	38.6782	38.6782	2843	53.3198	53.3198	-0.31044
1239	35.1994	35.1994	1962	44.2945	44.2945	-0.22587	1182	34.3802	34.3802	1917	43.7836	43.7836	-0.23717
1519	38.9743	38.9743	2760	52.5357	52.5357	-0.29002	1329	36.4555	36.4555	2696	51.923	51.923	-0.33963
2122	46.0652	46.0652	2967	54.4702	54.4702	-0.16604	922	30.3645	30.3645	1972	44.4072	44.4072	-0.36282
757	27.5136	27.5136	2035	45.111	45.111	-0.45774	1144	33.8231	33.8231	3100	55.6776	55.6776	-0.46089
1026	32.0312	32.0312	2046	45.2327	45.2327	-0.33203	1388	37.2559	37.2559	2800	52.915	52.915	-0.33715
777	27.8747	27.8747	1595	39.9375	39.9375	-0.34486	1421	37.6962	37.6962	2819	53.0943	53.0943	-0.32972
504	22.4499	22.4499	2011	44.8442	44.8442	-0.59921	836	28.9137	28.9137	2648	51.4587	51.4587	-0.52009
767	27.6948	27.6948	1833	42.8135	42.8135	-0.41	988	31.4325	31.4325	2574	50.7346	50.7346	-0.44526
853	29.2062	29.2062	1233	35.1141	35.1141	-0.18217	1129	33.6006	33.6006	1905	43.6463	43.6463	-0.25577
506	22.4944	22.4944	1887	43.4396	43.4396	-0.5771	805	28.3725	28.3725	2829	53.1883	53.1883	-0.55696
889	29.8161	29.8161	1262	35.5246	35.5246	-0.17341	1158	34.0294	34.0294	1682	41.0122	41.0122	-0.18451
728	26.9815	26.9815	2685	51.817	51.817	-0.5734	790	28.1069	28.1069	3041	55.1453	55.1453	-0.58758
2358	48.5592	48.5592	2950	54.3139	54.3139	-0.11153	1360	36.8782	36.8782	1827	42.7434	42.7434	-0.14653
1076	32.8024	32.8024	2953	54.3415	54.3415	-0.46587	1430	37.8153	37.8153	3541	59.5063	59.5063	-0.42466
909	30.1496	30.1496	1494	38.6523	38.6523	-0.24345	1552	39.3954	39.3954	2348	48.4562	48.4562	-0.2041
613	24.7588	24.7588	1889	43.4626	43.4626	-0.50999	1118	33.4365	33.4365	3104	55.7136	55.7136	-0.47039
728	26.9815	26.9815	1909	43.6921	43.6921	-0.44786	1113	33.3617	33.3617	2737	52.3163	52.3163	-0.42182
658	25.6515	25.6515	1864	43.1741	43.1741	-0.47819	1752	41.8569	41.8569	3146	56.0892	56.0892	-0.28461
598	24.454	24.454	1838	42.8719	42.8719	-0.50903	1014	31.8434	31.8434	2446	49.4571	49.4571	-0.41387
777	27.8747	27.8747	2095	45.7712	45.7712	-0.45891	1452	38.1051	38.1051	3243	56.9473	56.9473	-0.38147
817	28.5832	28.5832	1912	43.7264	43.7264	-0.40125	1246	35.2987	35.2987	2661	51.5849	51.5849	-0.36217
599	24.4745	24.4745	1851	43.0233	43.0232	-0.51102	1758	41.9285	41.9285	3221	56.7539	56.7539	-0.29383
551	23.4734	23.4734	1840	42.8952	42.8952	-0.53911	909	30.1496	30.1496	2319	48.156	48.156	-0.4368
670	25.8844	25.8844	1485	38.5357	38.5357	-0.37819	1332	36.4966	36.4966	2364	48.621	48.621	-0.27922
754	27.4591	27.4591	1631	40.3856	40.3856	-0.36772	1119	33.4515	33.4515	2312	48.0833	48.0833	-0.34771
604	24.5764	24.5764	2658	51.5558	51.5558	-0.62968	967	31.0966	31.0966	3478	58.9746	58.9746	-0.5649
619	24.8797	24.8797	1855	43.0697	43.0697	-0.4996	1043	32.2955	32.2955	2598	50.9706	50.9706	-0.42708
787	28.0535	28.0535	2190	46.7974	46.7974	-0.47128	1361	36.8917	36.8917	3038	55.1181	55.1181	-0.38122
596	24.4131	24.4131	2152	46.3897	46.3897	-0.56623	952	30.8545	30.8545	2431	49.3052	49.3052	-0.43719
937	30.6105	30.6105	2294	47.8957	47.8957	-0.41999	1384	37.2022	37.2021	3020	54.9545	54.9545	-0.37148
1041	32.2645	32.2645	1440	37.9473	37.9473	-0.16082	1328	36.4417	36.4417	2179	46.6798	46.6798	-0.24266
812	28.4956	28.4956	1913	43.7379	43.7379	-0.40404	1488	38.5746	38.5746	3214	56.6922	56.6922	-0.36708
1438	37.921	37.921	2121	46.0543	46.0543	-0.19191	1440	37.9473	37.9473	1910	43.7035	43.7035	-0.1403
749	27.3679	27.3679	2339	48.3632	48.3632	-0.5149	1238	35.1852	35.1852	2759	52.5262	52.5262	-0.38054
1459	38.1969	38.1969	1942	44.0681	44.0681	-0.14202	1319	36.318	36.318	1759	41.9404	41.9404	-0.14295
732	27.0555	27.0555	1572	39.6485	39.6485	-0.36458	1636	40.4475	40.4475	2816	53.066	53.066	-0.26505
1370	37.0135	37.0135	1952	44.1814	44.1814	-0.1752	1223	34.9714	34.9714	2022	44.9667	44.9667	-0.24623
517	22.7376	22.7376	1748	41.8091	41.8091	-0.54349	1116	33.4066	33.4066	2525	50.2494	50.2494	-0.38698
474	21.7715	21.7715	1803	42.4617	42.4618	-0.58366	814	28.5307	28.5307	1907	43.6692	43.6692	-0.40169
688	26.2298	26.2298	2249	47.4236	47.4236	-0.5315	837	28.931	28.931	3184	56.4269	56.4269	-0.58369
596	24.4131	24.4131	1959	44.2606	44.2606	-0.53346	1482	38.4968	38.4968	2761	52.5452	52.5452	-0.30144
698	26.4197	26.4197	1653	40.6571	40.6571	-0.40621	1646	40.5709	40.5709	2592	50.9117	50.9117	-0.22322

601	24.5153	24.5153	2123	46.076	46.076	-0.55874	1393	37.3229	37.3229	2729	52.2398	52.2398	-0.32412
528	22.9783	22.9783	1551	39.3827	39.3827	-0.49206	1376	37.0945	37.0945	2821	53.1131	53.1131	-0.34429
980	31.305	31.305	2112	45.9565	45.9565	-0.36611	1143	33.8083	33.8083	2155	46.422	46.422	-0.30685
596	24.4131	24.4131	1677	40.9512	40.9512	-0.47558	1361	36.8917	36.8917	2993	54.7083	54.7083	-0.37483
1019	31.9218	31.9218	1999	44.7102	44.7102	-0.32472	1259	35.4824	35.4824	2178	46.669	46.669	-0.26738
836	28.9137	28.9137	1697	41.1947	41.1947	-0.33991	1226	35.0143	35.0143	2927	54.1018	54.1018	-0.40958
1053	32.45	32.45	1936	44	44	-0.29542	1279	35.7631	35.7631	2574	50.7346	50.7346	-0.3361
839	28.9655	28.9655	1550	39.37	39.37	-0.29761	1789	42.2966	42.2966	2823	53.1319	53.1319	-0.2242
988	31.4325	31.4325	1802	42.45	42.45	-0.29176	1430	37.8153	37.8153	2479	49.7896	49.7896	-0.26836
1530	39.1152	39.1152	2581	50.8035	50.8035	-0.25566	2439	49.3862	49.3862	3280	57.2713	57.2713	-0.14705
799	28.2666	28.2666	1611	40.1373	40.1373	-0.33693	1177	34.3074	34.3074	2212	47.0319	47.0319	-0.3054
614	24.779	24.779	2325	48.2183	48.2183	-0.58217	1118	33.4365	33.4365	3262	57.1139	57.1139	-0.4895
1095	33.0908	33.0908	1879	43.3474	43.3474	-0.26362	1389	37.2693	37.2693	2692	51.8845	51.8845	-0.31928
623	24.96	24.96	1682	41.0122	41.0122	-0.45944	2188	46.7761	46.7761	3354	57.9137	57.9137	-0.21039
534	23.1084	23.1084	1718	41.4488	41.4488	-0.52576	1004	31.686	31.686	2314	48.1041	48.1041	-0.39482
685	26.1725	26.1725	1987	44.5758	44.5758	-0.48728	1538	39.2173	39.2173	3150	56.1249	56.1249	-0.34386
762	27.6043	27.6043	1643	40.5339	40.5339	-0.36632	1271	35.6511	35.6511	2827	53.1695	53.1695	-0.3797
932	30.5287	30.5287	1742	41.7373	41.7373	-0.30292	1810	42.5441	42.5441	3023	54.9818	54.9818	-0.25098
1029	32.078	32.078	2061	45.3982	45.3982	-0.33398	1350	36.7423	36.7423	2641	51.3907	51.3907	-0.32348
845	29.0689	29.0689	1554	39.4208	39.4208	-0.29554	1152	33.9411	33.9411	2170	46.5833	46.5833	-0.30644
1229	35.0571	35.0571	2082	45.6289	45.6289	-0.25763	1116	33.4066	33.4066	2599	50.9804	50.9804	-0.39919
712	26.6833	26.6833	1368	36.9865	36.9865	-0.31539	1419	37.6696	37.6696	2280	47.7493	47.7493	-0.23277
993	31.5119	31.5119	1864	43.1741	43.1741	-0.30487	1422	37.7094	37.7094	2601	51	51	-0.29307
829	28.7924	28.7924	1661	40.7554	40.7554	-0.33414	1545	39.3065	39.3065	2917	54.0093	54.0093	-0.30749
1678	40.9634	40.9634	2170	46.5833	46.5833	-0.12786	1348	36.7151	36.7151	1951	44.1701	44.1701	-0.18278
597	24.4336	24.4336	1670	40.8656	40.8656	-0.47331	728	26.9815	26.9815	2789	52.811	52.811	-0.58601
1175	34.2783	34.2783	1836	42.8486	42.8486	-0.21953	1326	36.4143	36.4143	2454	49.5379	49.5379	-0.29841
911	30.1828	30.1828	2729	52.2398	52.2398	-0.49945	1704	41.2795	41.2795	3312	57.55	57.55	-0.32057
793	28.1603	28.1603	1990	44.6094	44.6094	-0.43011	1285	35.8469	35.8469	2575	50.7445	50.7445	-0.3342
859	29.3087	29.3087	2242	47.3498	47.3498	-0.44599	1302	36.0832	36.0832	2970	54.4977	54.4977	-0.39045
506	22.4944	22.4944	1665	40.8044	40.8044	-0.53386	1080	32.8634	32.8634	2554	50.5371	50.5371	-0.40561
533	23.0868	23.0868	1772	42.0951	42.0951	-0.53753	1015	31.8591	31.8591	2904	53.8888	53.8888	-0.48201
873	29.5466	29.5466	2118	46.0217	46.0217	-0.41625	1200	34.641	34.641	2857	53.4509	53.4509	-0.40843
804	28.3549	28.3549	1779	42.1782	42.1782	-0.37747	1388	37.2559	37.2559	2914	53.9815	53.9815	-0.35472
888	29.7993	29.7993	1829	42.7668	42.7668	-0.34634	1338	36.5787	36.5787	2457	49.5681	49.5681	-0.29486
1949	44.1475	44.1475	3495	59.1185	59.1185	-0.28398	1476	38.4187	38.4187	3573	59.7746	59.7746	-0.41533
1673	40.9023	40.9023	3109	55.7584	55.7584	-0.30029	1506	38.8072	38.8072	2462	49.6185	49.6185	-0.24093
1044	32.311	32.311	2253	47.4658	47.4658	-0.3667	1916	43.7721	43.7721	3247	56.9825	56.9825	-0.2578
790	28.1069	28.1069	2152	46.3897	46.3897	-0.46295	1361	36.8917	36.8917	2821	53.1131	53.1131	-0.34912
1108	33.2866	33.2866	1428	37.7889	37.7889	-0.12618	1370	37.0135	37.0135	1776	42.1426	42.1426	-0.12905
962	31.0161	31.0161	1872	43.2666	43.2666	-0.3211	1651	40.6325	40.6325	2715	52.1057	52.1057	-0.2437
780	27.9285	27.9285	1856	43.0813	43.0813	-0.40819	1267	35.5949	35.5949	3337	57.7668	57.7668	-0.44961
1087	32.9697	32.9697	2435	49.3457	49.3457	-0.38274	1259	35.4824	35.4824	2575	50.7445	50.7445	-0.34325
961	31	31	2053	45.31	45.31	-0.36231	1126	33.5559	33.5559	2971	54.5069	54.5069	-0.45033
1626	40.3237	40.3237	2045	45.2217	45.2217	-0.11414	1288	35.8887	35.8887	1830	42.7785	42.7785	-0.17383

Data(B): Enhancement of cervical x-ray radiograph:

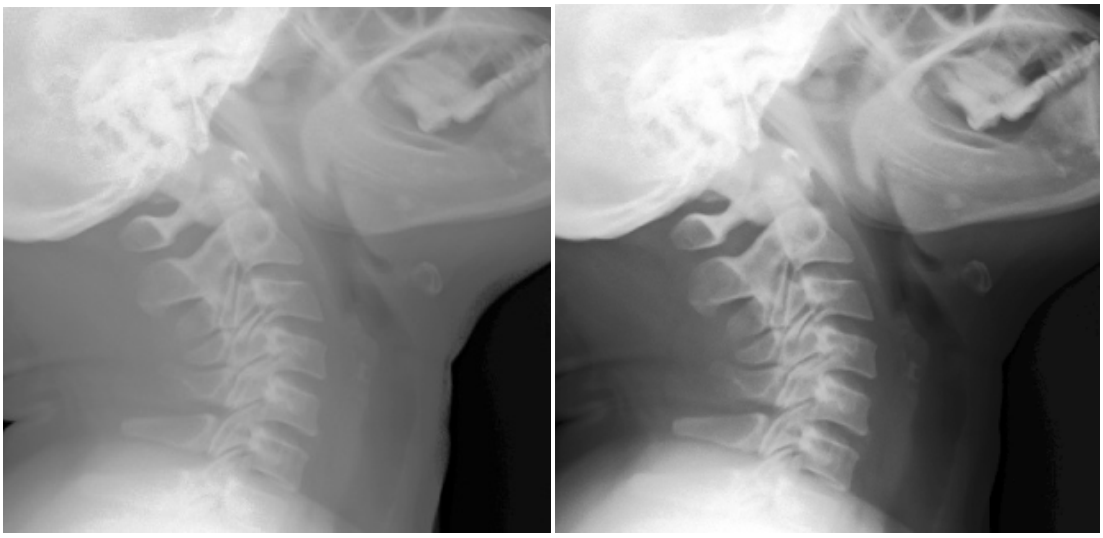

A B

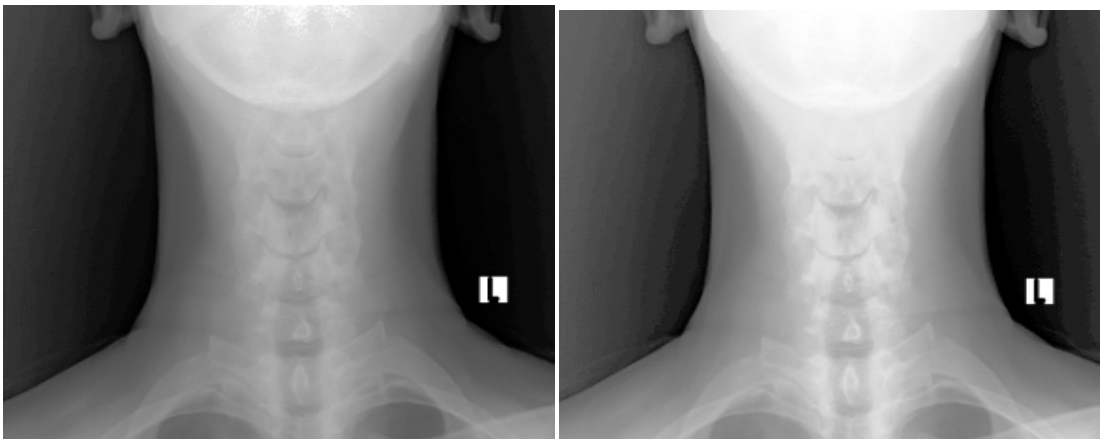

C D

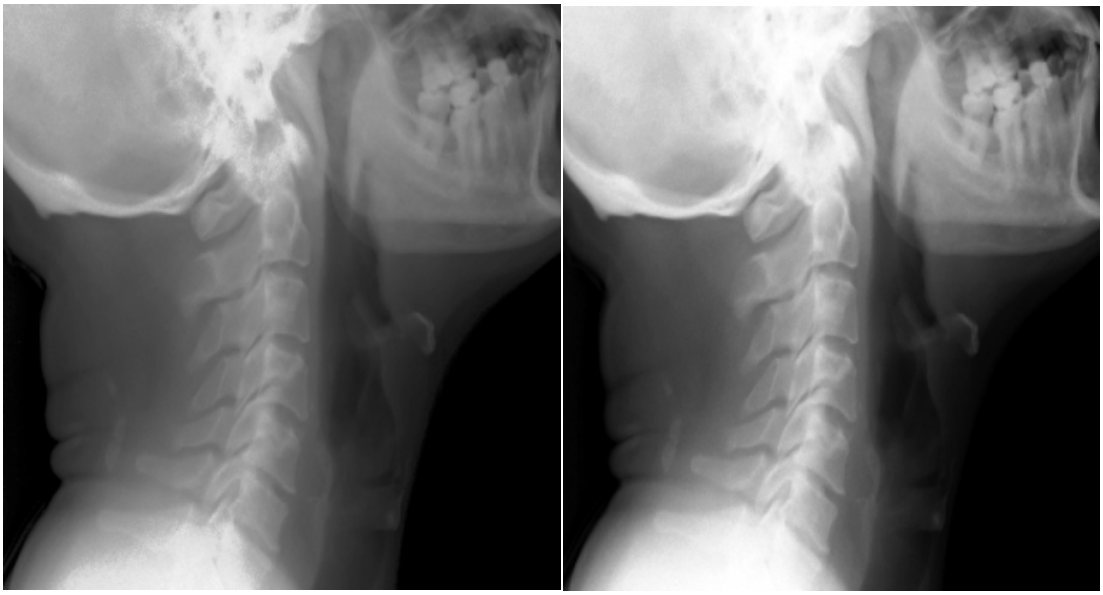

E F

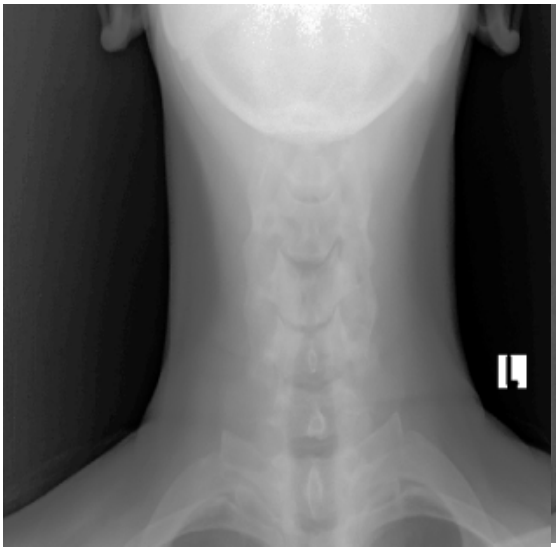

G

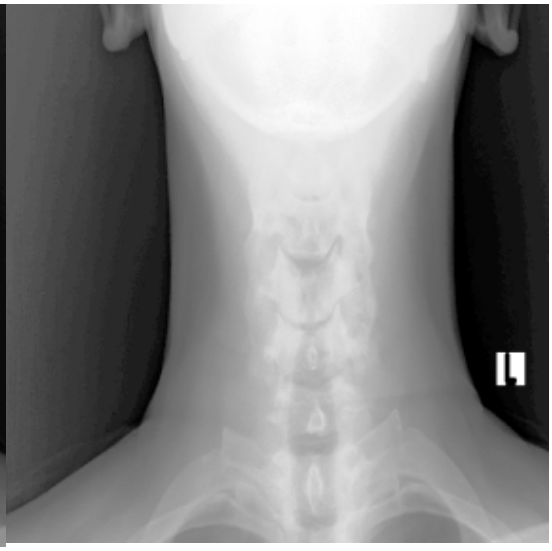

H

I

J

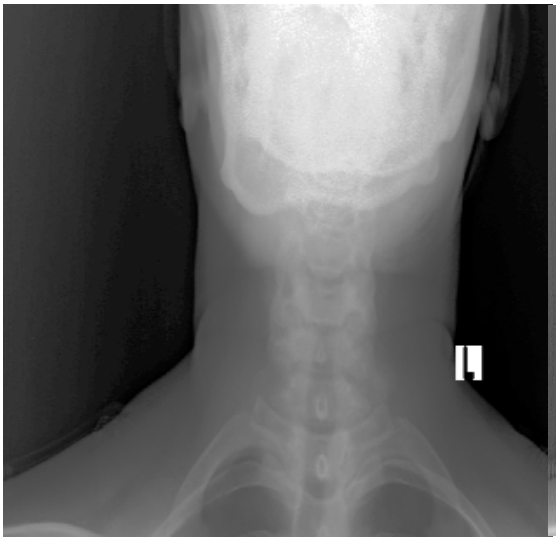

K

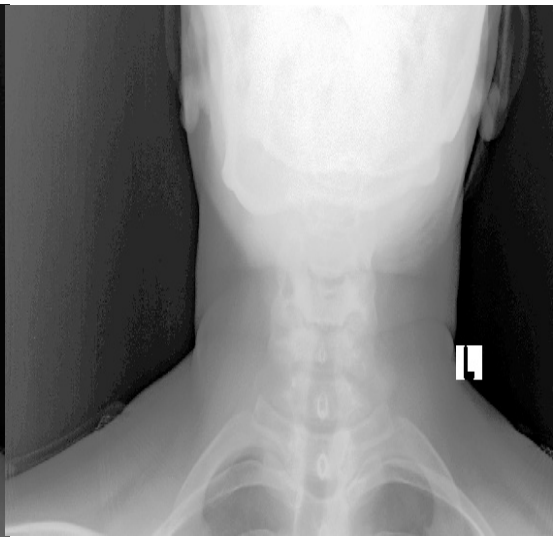

L

M

N

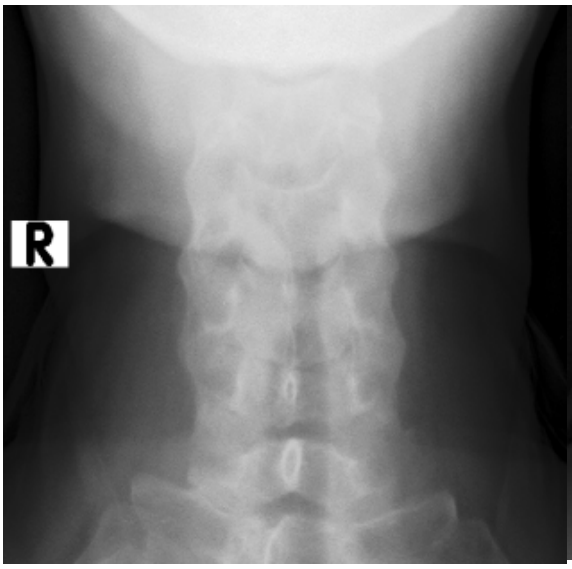

O

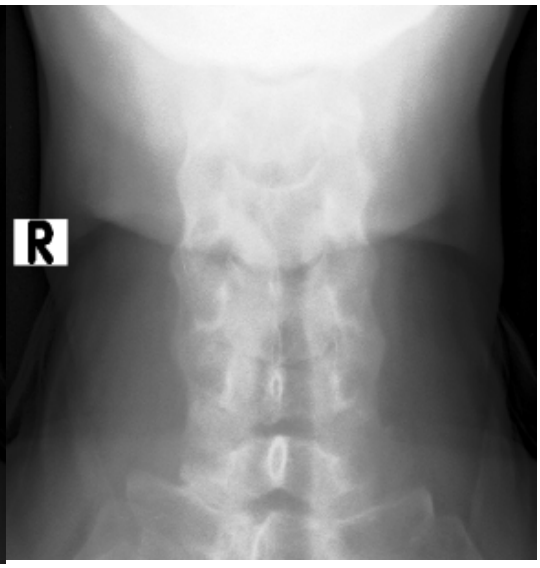

P

Q

R

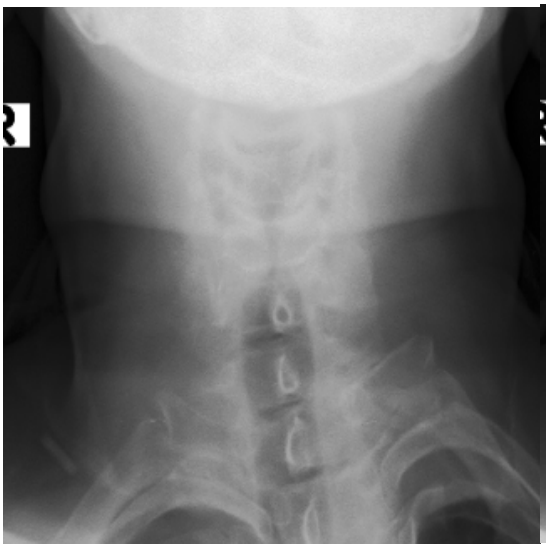

S

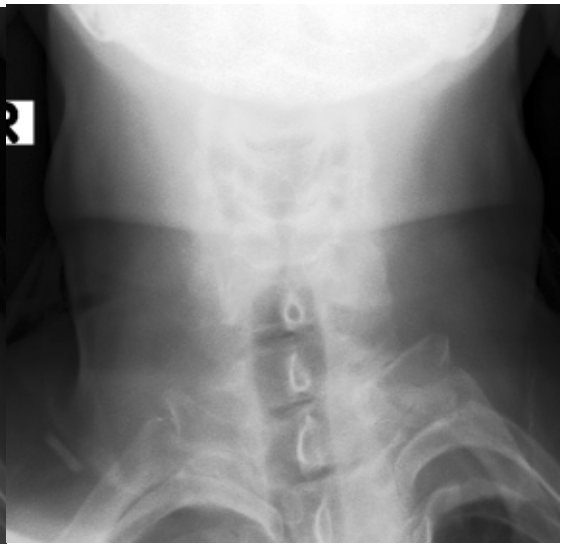

T

U

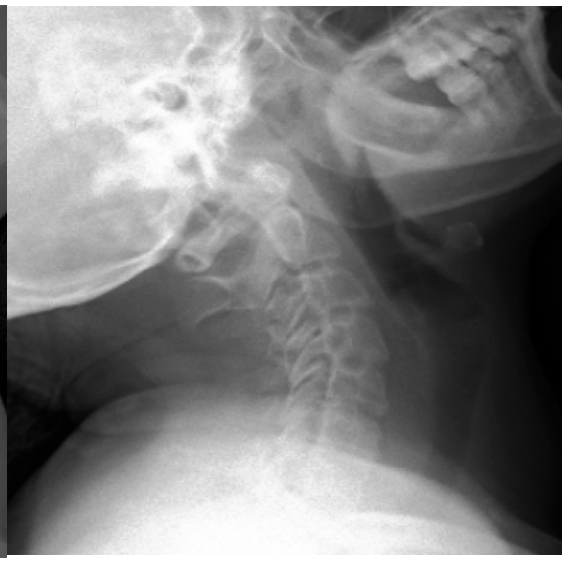

V

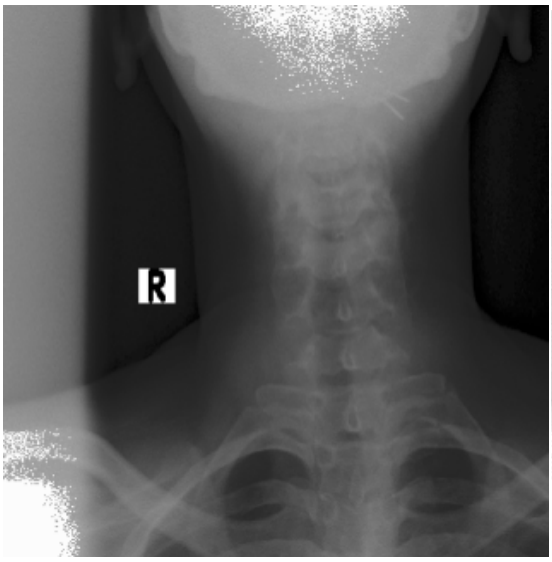

W

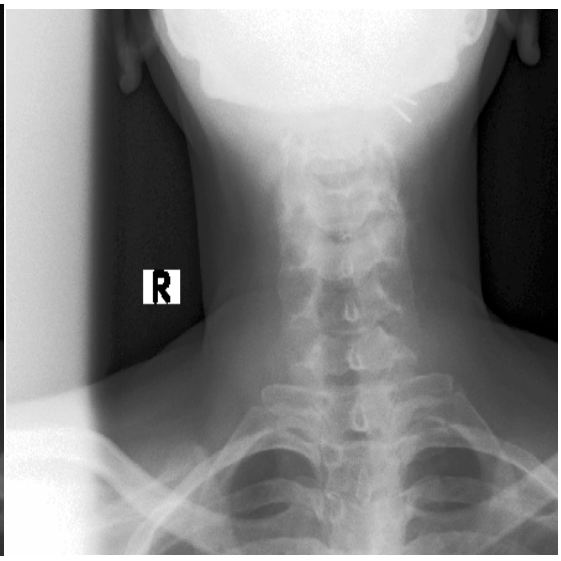

X

Y

Z

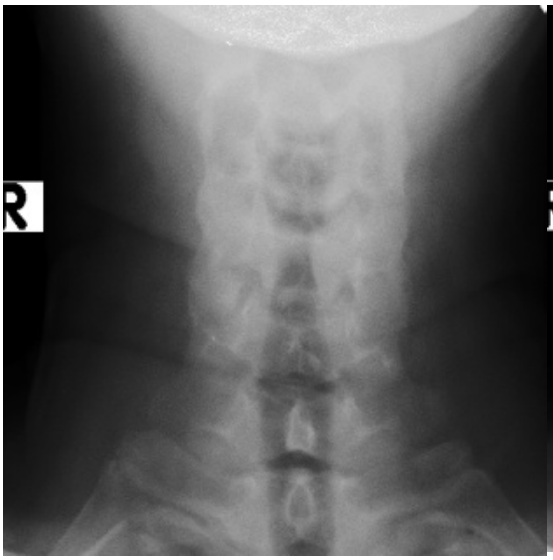

AA

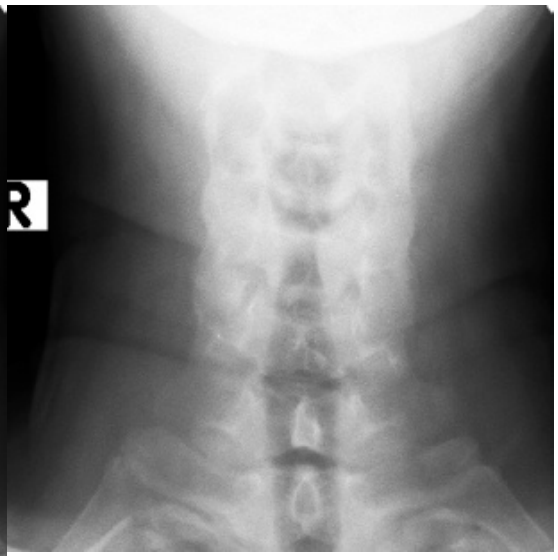

BB

CC

DD